



The KBTBD6/7-DRD2 axis regulates pituitary adenoma sensitivity to dopamine agonist treatment

Yan Ting Liu¹ · Fang Liu^{2,6} · Lei Cao³ · Li Xue¹ · Wei Ting Gu¹ · Yong Zhi Zheng^{1,4} · Hao Tang¹ · Yu Wang⁵ · Hong Yao¹ · Yong Zhang¹ · Wan Qun Xie^{1,4} · Bo Han Ren^{1,4} · Zhuo Hui Xiao² · Ying Jie Nie⁶ · Ronggui Hu^{2,7,8} · Zhe Bao Wu^{1,4}

Received: 8 March 2020 / Revised: 12 June 2020 / Accepted: 12 June 2020 / Published online: 22 June 2020
© Springer-Verlag GmbH Germany, part of Springer Nature 2020

Abstract

Pituitary adenoma (PA) is one of the most common intracranial tumors, and approximately 40% of all PAs are prolactinomas. Dopamine agonists (DAs), such as cabergoline (CAB), have been successfully used in the treatment of prolactinomas. The expression of dopamine type 2 receptor (DRD2) determines the therapeutic effect of DAs, but the molecular mechanisms of DRD2 regulation are not fully understood. In this study, we first demonstrated that DRD2 underwent proteasome-mediated degradation. We further employed the yeast two-hybrid system and identified kelch repeat and BTB (POZ) domain containing 7 (KBTBD7), a substrate adaptor for the CUL3-RING ubiquitin (Ub) ligase complex, as a DRD2-interacting protein. KBTBD6/7 directly interacted with, and ubiquitinated DRD2 at five ubiquitination sites (K221, K226, K241, K251, and K258). CAB, a high-affinity DRD2 agonist, induced DRD2 internalization, and cytoplasmic DRD2 was degraded via ubiquitination under the control of KBTBD6/7, the activity of which attenuated CAB-mediated inhibition of the AKT/mTOR pathway. KBTBD7 knockout (KO) mice were generated using the CRISPR-Cas9 technique, in which the static level of DRD2 protein was elevated in the pituitary gland, thalamus, and heart, compared to that of WT mice. Consistently, the expression of KBTBD6/7 was negatively correlated with that of DRD2 in human pituitary tumors. Moreover, KBTBD7 was highly expressed in dopamine-resistant prolactinomas, but at low levels in dopamine-sensitive prolactinomas. Knockdown of KBTBD6/7 sensitized MMQ cells and primary pituitary tumor cells to CAB treatment. Conversely, KBTBD7 overexpression increased CAB resistance of estrogen-induced *in situ* rat prolactinoma model. Together, our findings have uncovered the novel mechanism of DRD2 protein degradation and shown that the KBTBD6/7-DRD2 axis regulates PA sensitivity to DA treatment. KBTBD6/7 may thus become a promising therapeutic target for pituitary tumors.

Keywords Pituitary tumor · DRD2 · KBTBD7 · KBTBD6 · Ubiquitin degradation

Introduction

Pituitary adenoma (PA) is a common intracranial tumor, and approximately 40% of all PAs are prolactinomas [15]. Dopamine agonists (DAs), such as bromocriptine (BCR) and cabergoline (CAB), are first-line treatments for prolactinomas [4, 7, 15, 29, 63], as they can effectively decrease the secretion of serum prolactin (PRL) and have been shown to markedly shrink tumor size in approximately 90% of patients [8, 38]. The mechanism of DAs primarily involves their activation of dopamine type 2 receptor (DRD2) on the surface of pituitary tumor cells. Dopamine receptors (DRs) belong to the G-protein-coupled receptor (GPCR) superfamily [23] and are classified as D1-like (D1 and D5 receptors) or D2-like (D2, D3, and D4 receptors) that activate (via

Yan Ting Liu, Fang Liu, Lei Cao, and Li Xue have contributed equally to this work.

Electronic supplementary material The online version of this article (<https://doi.org/10.1007/s00401-020-02180-4>) contains supplementary material, which is available to authorized users.

✉ Ronggui Hu
coryhu00@gmail.com

✉ Zhe Bao Wu
zhebaowu@aliyun.com

Extended author information available on the last page of the article

Gs-proteins) or inhibit (via Gi/o-proteins) adenylate cyclase (AC), respectively [2, 51].

However, 10–20% of prolactinomas are resistant to DA treatment [8, 39], which is primarily associated with the low expression of DRD2 [6, 42, 56]. However, the mechanism of DRD2 downregulation is largely unknown. DNA methylation was suggested to play a role in the regulation of DRD2 expression in the GH3 rat pituitary cell line [44]. Meanwhile, although exogenous DRD2 can be ubiquitinated [25], the mechanism of this ubiquitination remains completely unknown. In addition to its role in PAs, DRD2 plays a crucial role in human memory and activity and is correlated with craniocerebral diseases, such as Parkinson's disease, schizophrenia, and attention deficit hyperactivity disorder (ADHD), making it the primary target to treat Parkinson's disease and hyperprolactinemia [3, 9, 11, 13, 24, 26, 30, 37, 49, 50].

Ubiquitin signaling governs multiple biological processes, including apoptosis and autophagy, and disease conditions, such as cancer [18, 33, 43, 53]. Ubiquitination, the reaction by which Ub is attached to a substrate protein, regulates the stability, function, and protein–protein interactions of the substrate. For example, KBTBD2 was shown to mediate p85 α ubiquitination and degradation, activate the phosphatidylinositol 3-kinase (PI3K) pathway, and promote insulin sensitivity [62]. KBTBD6 and KBTBD7, substrate adaptors for the Cullin-RING ligase (CRL) complex, were reported to specifically bind GABARAP proteins, ubiquitylate TIAM1 and target the protein for proteasomal degradation, thus inhibiting RAC1 signaling [14]. In addition, KBTBD7 regulates the degradation of neurofibromin and increase the proliferation of glioblastoma [19]. However, the roles of KBTBD6/7 in DRD2 regulation and in PA treatment remain completely unknown.

In this study, we performed yeast two-hybrid screening and identified a BTB-Kelch protein, KBTBD7, as a novel interaction partner of DRD2. We showed that CAB induces DRD2 internalization and that KBTBD6/7 targets internalized DRD2 at the K221, K226, K241, K251, and K258 sites, and promotes its proteasomal degradation. As a result, KBTBD6/7 depletion stabilizes DRD2 and promotes prolactinoma cell sensitivity to DA treatment. Moreover, we observed that KBTBD6/7 was highly expressed in dopamine-resistant prolactinomas and negatively correlated with DRD2 expression in pituitary tumors.

Materials and methods

Plasmids

See Supplementary information (Suppl. Table 1) for details. ShRNAs targeting different regions of KBTBD6

or KBTBD7 were cloned into the pLKO.1 lentiviral vector. Adenoviruses expressing rat Flag-KBTBD7 and human KBTBD7 and KBTBD6 knockdown adenoviruses were purchased from Vigene Biosciences. The shRNA-targeted sequences are provided in Suppl. Table 2.

Cell culture and reagents

HEK293T cells were kindly provided by the Ronggui Hu's laboratory. The MMQ rat pituitary cell line was purchased from the American Type Culture Collection (ATCC, CRL-10609™) and was shown to be free of mycoplasma contamination (tested using a Mycoplasma Stain Assay kit, Beyotime, cat no. C0296, China). HEK293T cells were cultured in Dulbecco's modified Eagle's medium (DMEM, Gibco, 11965-118) supplemented with 10% (v/v) fetal bovine serum (FBS, Moregate, FBS500), 100 U/ml penicillin, and 100 µg/ml streptomycin (Gibco, 15140122). MMQ cells were cultured in Ham's F-12K (Kaighn's) medium (Gibco, 21127022) supplemented with 2.5% fetal bovine serum, 15% horse serum (Bioworld, 04-004-1A), and 1% penicillin/streptomycin. For primary pituitary tumor cell cultures, PA tissues freshly isolated from surgeries were enzymatically and mechanically dispersed, and the obtained tumor cells were carefully washed by repeated centrifugation and cultured in DMEM supplemented with 10% FBS and 1% penicillin/streptomycin. All cell lines were maintained in a humidified atmosphere with 5% CO₂ at 37 °C.

Ubiquitination assay

An in vivo ubiquitination assay was performed as described previously [33]. Briefly, HEK293T cells were co-transfected with the indicated plasmids or shRNA for 48 h, followed by MG132 treatment for 6 h before harvesting and lysis. IP was carried out using anti-flag beads. After incubation with rotation, the anti-flag beads were washed with RIPA lysis buffer [50 mM Tris–Cl (pH 7.4), 150 mM NaCl, 5 mM EDTA, 1% (v/v) Triton X-100, 0.5% sodium pyrophosphate, 0.1% SDS, and protease inhibitor cocktail (Roche, 4693159001)] and boiled for 10 min in SDS-PAGE sample buffer, immunoblotted with the indicated antibodies.

Cycloheximide chase assay

HEK293T cells were seeded in 6-well plates, and then treated with cycloheximide (CHX, 100 µg/ml, ApexBio, A8244) for the indicated time. Then, the cells were lysed in RIPA buffer (150 mM NaCl, 50 mM Tris, and 1% Triton X-100, pH 7.5) supplemented with protease inhibitor cocktail and sonicated using a Vibra-Cell processor, resolved by SDS-PAGE and immunoblotted with the indicated antibodies.

Stable cell lines

Stable MMQ and HEK293T cell lines were generated through transduction with packaged lentivirus. Briefly, HEK293T cells in 6-cm dishes were transfected with pLVX-Myc-KBTBD7 or pLKO.1-shKBTBD6/7 and the packaging plasmids pMD2.G and pSPAX2. Virus-containing media were collected at 48 and 72 h after transfection, mixed, filtered through 0.45-μm nitrocellulose filters (Millipore, SLH-V033RS), and used to infect HEK293T or MMQ cells in the presence of 5 mg/ml polybrene (Sigma, 107689). Stably infected cells among the transduced cells were selected with puromycin (2 μg/ml) in bulk cultures.

Yeast two-hybrid (Y2H) screening

Y2H screening was performed as previously described [33] using DRD2 as the bait protein. Both pGBK7-DRD2 and the human ORFeome library (pACT2 backbone) were co-transformed into the yeast strain AH109. Positive colonies survived in SD-4 medium (deficient in Ade, His, Leu and Trp; Clontech, 630425) and showed a blue color in the presence of X-Gal (Sigma, B4252).

Immunoblotting (IB) analysis and immunoprecipitation (IP)

Standard immunoprecipitation (IP) was performed with the indicated antibodies, and the samples were scanned using ImageJ for normalization when needed as described previously. For IP analysis, the cells were lysed in Triton X-100 lysis buffer (150-mM NaCl, 50-mM Tris and 1% Triton X-100, pH 7.5) supplemented with protease inhibitor cocktail and sonicated using a Vibra-Cell processor. Then, the whole-cell lysates were incubated with anti-flag antibody-conjugated agarose beads or antibody (1–2 μg) for 3–4 h at 4 °C, followed by a 1-h incubation with protein A-Sepharose beads (GE Healthcare, 17051010) if free antibody was used. Immunoprecipitates were washed five times with washing buffer (150 mM NaCl, 50 mM Tris and 1% Triton X-100, pH 7.5), resolved by SDS-PAGE and immunoblotted with the indicated antibodies. Information on the antibodies used in this study is provided in Suppl. Table 3.

Immunofluorescence microscopy

Cells were co-transfected with the Flag-DRD2 vector and the Myc-KBTBD7 or Myc-KBTBD6 vector for 48 h. Then, the cultured cells were washed with PBS once, fixed with cold 4% formaldehyde for 30 min, and then rinsed with PBS three times. The cells were then permeabilized with cold 0.2% Triton X-100 for 15 min and incubated with primary antibodies overnight at 4 °C after 3% BSA blocking.

Subsequently, the cells were incubated with secondary antibodies conjugated with Alexa 488 (CST, 4412S) or Alexa 555 (CST, 4409S) in 5% BSA for 1 h at 37 °C. Nuclei were stained with DAPI (Vector Laboratories), and a confocal microscope (Nikon, Tokyo, Japan) was used to observe all stained slices.

GST pulldown assay

GST and GST-DRD2 were expressed in BL21 competent cells and purified using glutathione-agarose beads (GE Healthcare, 17075601) according to the manufacturer's instructions. The KBTBD6-His6 and KBTBD7-His6 proteins were purified using Ni-NTA agarose beads (Qiagen, 18735328) following the manufacturer's protocols. Purified KBTBD7-His6 and GST-DRD2 proteins were incubated in pulldown buffer [50-mM Tris-Cl (pH 8.0), 200-mM NaCl, 1-mM EDTA, 1% NP-40, 1-mM DTT, and 10-mM MgCl₂] for 2 h at 4 °C. Subsequently, the beads were washed five times with pulldown buffer and analyzed by immunoblotting. Pulldown assays to assess other proteins were carried out following the same procedures.

RNA extraction and qRT-PCR

Total RNA was purified from cells using TRIzol reagent (Invitrogen, 15596018) according to the manufacturer's instructions, and the RNA concentration was assessed using a NanoDrop 1000 spectrophotometer. Equal amounts of RNA (500 ng) were reverse transcribed using a cDNA synthesis kit (TaKaRa, RR036A). Complementary DNA (cDNA) was diluted (1:10 final dilution) and used for qRT-PCR analyses with SYBR Green Supermix reagent (TaKaRa, RR820A). The sequences of the primers used for qRT-PCR are provided in Suppl. Table 4.

DERET assay

DRD2 internalization was measured in real time in 96-well culture cell plates using SNAP-DRD2-transfected HEK293 cells. Cells were labeled with Lumi4-Tb in HBSS buffer for 1 h at 4 °C. Excess SNAP-Lumi4-Tb was then removed by washing each well four times with 100 μl of HBSS buffer. Internalization experiments were performed by incubating cells with 100 μl of HBSS buffer with or without agonist in the presence of 24 μM fluorescein. Ten microliters of antagonist were added at a specific time. TR fluorescence was serially read using an Infinite 500-multimode microplate reader (Tecan) with an excitation wavelength of 340 nm and a 150-μs delay and 400-μs integration time (for emission at 520 nm) or a 1500-μs delay and 1500-μs integration time (for emission at 620 nm). A value representing surface receptor internalization was calculated by dividing

the 620-nm signal by the 520-nm signal and multiplying the resultant number by 10,000.

cAMP assays

HEK293T cells transfected with empty vector and HEK293T cells expressing Myc-KBTBD7 or shKBTBD6/7 were seeded in 6-well plates. The cells were treated with or without CAB (20 μM) for 2 h. Then, the cAMP level was determined using an ELISA kit from Panchao Biological Technology Co. (Shanghai, PCDBA0101, China).

Plasma membrane protein isolation, and cell fractionation assay

Plasma membrane, cytoplasm, and nucleus proteins were isolated from HEK393T cells by Minute™ plasma membrane protein isolation kit (Invent Biotechnologies, SM-005) and resolved by SDS-PAGE and immunoblotted with the indicated antibodies.

Generation and validation of CRISPR-mediated KBTBD7 knockout mice

CRISPR-mediated KBTBD7 KO mice were produced by Beijing View Solid Biotechnology, China. Linear pCAG-T7-Cas9 plasmid that had been cut with the restriction enzyme *Not I* was used as the in vitro transcriptional template. After gel purification, Cas9 mRNA was transcribed using a mMESSAGE mMACHINE T7 Ultra kit (Life Technologies, AMB13455). KBTBD7-gRNA templates (KBTBD7-L2: GGAAACAGTGAGTCAGCC; and KBTBD7-R3: TGAAATAATCGGATTCA) based on the gRNA scaffold were expressed from the T7 promoter and transcribed with a fast transcription T7 kit (cat. No. VK010, Beijing View Solid Biotechnology, China). Then, the transcribed gRNAs were frozen at –80 °C. C57BL/6 mouse zygotes were injected with Cas9 mRNA and KBTBD7-gRNA in M2 medium (Millipore, MR-015P-D) using a Femtojet micromanipulator (Eppendorf, Germany). After microinjection, the zygotes were transferred to pseudopregnant females. All mice were maintained in a specific pathogen-free facility. Tail-derived DNA from 2-week-old newborn mice was genotyped by sequencing PCR-amplified products with the following primers: forward (AAGATGCAAAGCGGC TTCGG), reverse 1 (GTTTCCTGTGACCTTGTAAAG), and reverse 2 (ACTTGAGGATGGCAGTGCAA). The mutant mice were mated with WT C57BL/6 mice to obtain heterozygous KBTBD7[±] mice, which were then intercrossed to generate homozygous KBTBD7 KO mice (KBTBD7^{–/–}) and littermate controls.

Immunohistochemistry (IHC)

Antigens were retrieved from formaldehyde-fixed, paraffin-embedded (FFPE) tumor tissue sections by boiling in sodium citrate buffer (pH 6.0) for 30 min using a microwave histoprocessor. The tissue sections were dehydrated and subjected to peroxidase blocking. IHC staining was performed by incubating the tissue sections with primary antibodies overnight at 4 °C followed by incubation with goat anti-mouse horseradish peroxidase-conjugated secondary antibody (ab6788, Abcam; 1:200 in 1% BSA/TBST) for 1 h at room temperature. The sections were then exposed to DAB substrate (dissolved in Dako substrate buffer, 760–500, Roche, Indianapolis, IN, USA) followed by counterstaining with Gill's hematoxylin and standard dehydration treatment. Images of the stained sections were obtained using an Axiovert 200 microscope (Carl Zeiss, Oberkochen, Germany). The expression of KBTBD6, KBTBD7, and DRD2 was measured by determining the integrated optical density (sum) of each image using Image-Pro Plus 5.1 (Diagnostic Instruments, Sydney, NSW, Australia). Expression in each sample was quantified in ten random fields (400×) per case by two independent observers who were blinded to the patients' clinical features.

Cell proliferation assays

Ten thousand cells per well were seeded in triplicate in 96-well plates, and after 24, 48, and 72 h, the number of viable cells was measured with a Cell Counting Kit-8 kit (Bimake, B34304). After the addition of CCK8 solution, the plate was incubated at 37 °C for 1–4 h, and the absorbance at 450 nm was determined with a plate reader (Tecan, Switzerland).

Colony formation assay

Six-well plates were pretreated with poly-D-lysine (Thermo Fisher, A3890401). Then, 1000 cells/well were seeded in 6-well plates and grown for 2 weeks. After fixation with 4% paraformaldehyde, the fixed cells were stained with a 1% crystal violet staining solution (Sangon Biotech, E607309-0100) for 15 min at room temperature. The plates were then imaged after extensive washing and air drying.

Isolation and cultivation of pituitary adenomas

Pituitary adenomas were obtained from surgery and then transferred to DMEM. The tissues were washed three times with HBSS (Gibco, 14025092) and cut into small pieces of about 3–4 mm by sterile scalpel, and rinsed and digested with HBSS containing 100 U/ml collagenase, type IV (Gibco, 17104019) at 37 °C for 6–8 h. The dispersed cells

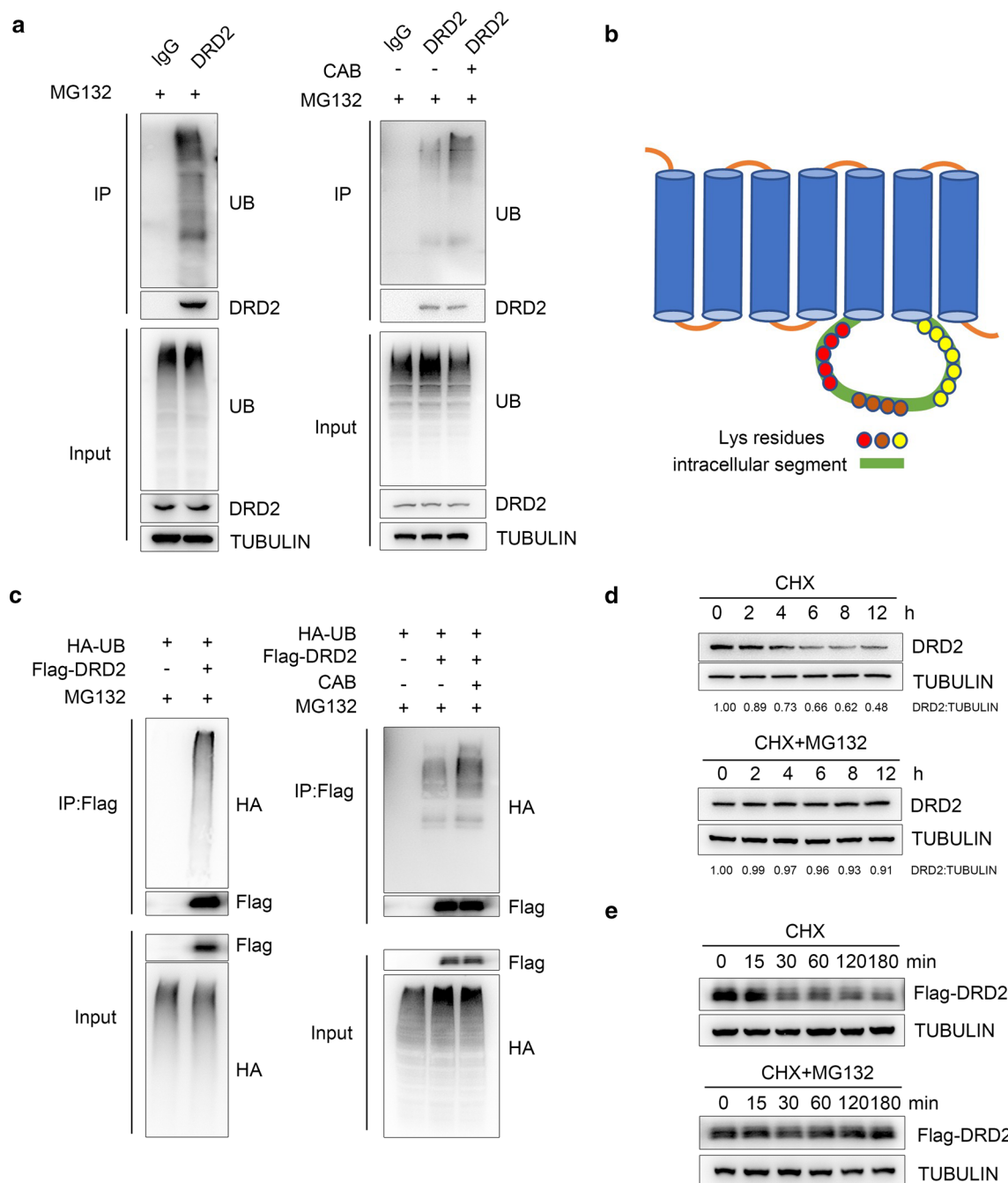


Fig. 1 DRD2 is regulated by a proteasome-mediated protein degradation pathway. **a** Endogenous DRD2 was ubiquitinated, and cabergoline promoted the ubiquitination of DRD2 in HEK293T cells. **b** Schematic representation of the intracellular segment of DRD2. **c** Flag-tagged DRD2 was ubiquitinated, and CAB promoted the ubiquitination of Flag-tagged DRD2 in HEK293T cells. **d**, **e** Endogenous

DRD2 and an intracellular segment of DRD2 with a Flag tag underwent proteasome-dependent degradation in HEK293T cells. The protein levels measured in CHX chase experiments indicated that endogenous DRD2 (**d**) and the intracellular segment of Flag-tagged DRD2 (**e**) were degraded in HEK293T cells, and this reduction was reversed by MG132 treatment

can be sieved using 100-μm cell strainer (Beyotime Biotechnology, FSTR100). These cells were washed with HBSS and resuspended in ACK Lysing Buffer (Gibco, A1049201).

About 5 min later, the cells were resuspended in DMEM with 10% FBS and seeded in 10-cm cell culture dish for experiments.

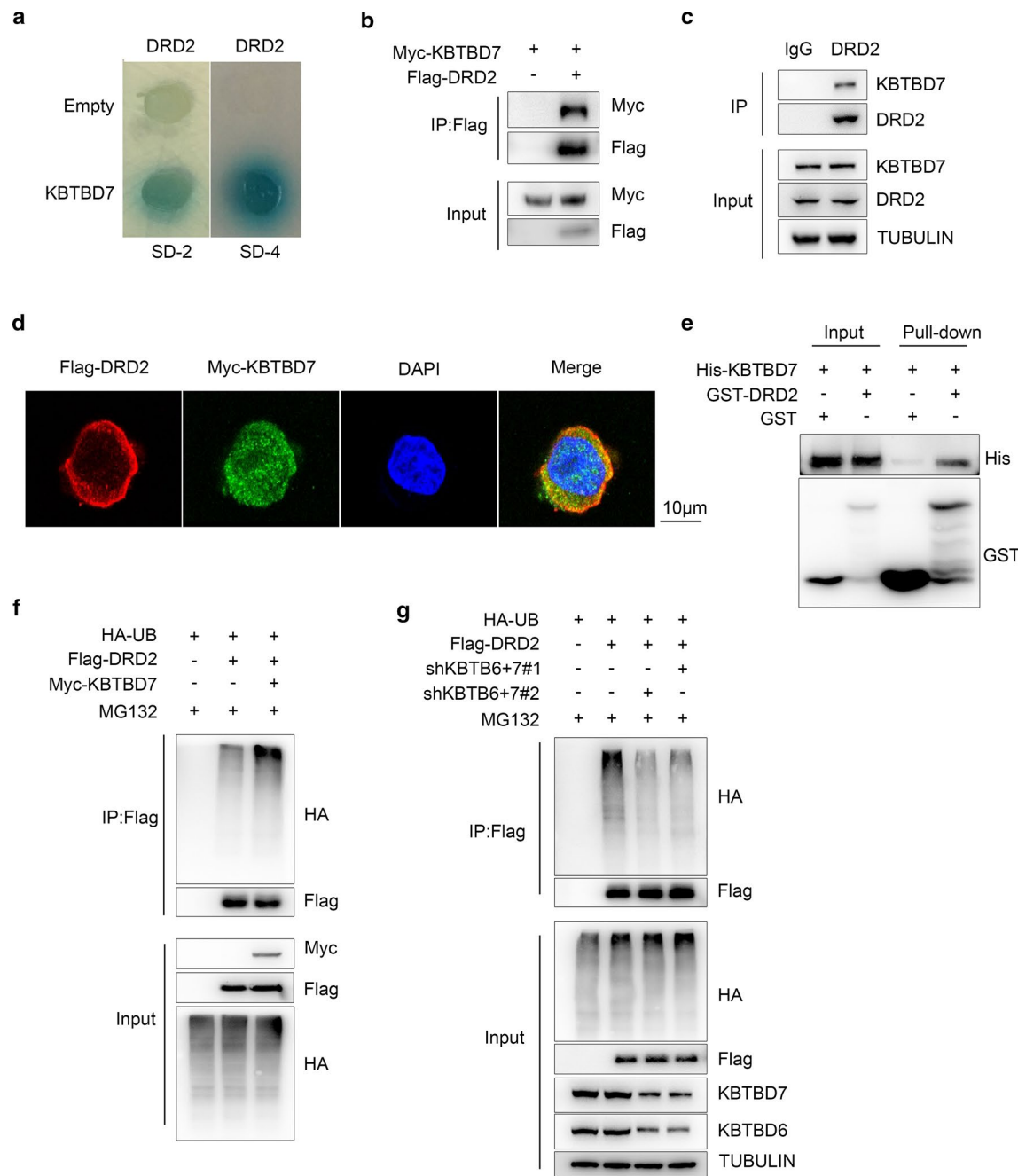


Fig. 2 KBTBD7 directly interacts with and ubiquitinates DRD2. **a** Human DRD2 was shown to interact with KBTBD7 in a yeast two-hybrid system. When DRD2 was used as bait, KBTBD7 interacted with DRD2 in yeast. Co-transformation of DRD2 and KBTBD7 into the yeast strain Mav 203 activated the expression of β-glycosidase. SD-2: deficient in Leu, Trp; SD-4: deficient in Leu, Trp, His, and Ura. **b–e** KBTBD7 interacted with DRD2. Coimmunoprecipitation assays showed that tagged (**b**) or endogenous DRD2 (**c**) and KBTBD7 formed a complex in HEK293T cells. Immunofluorescence

microscopy analyses indicated that tagged KBTBD7 and DRD2 proteins were colocalized in MMQ cells (**d**). Scale bar: 10 μm. GST pulldown assays indicated that only recombinant GST-tagged DRD2, but not GST, interacted with His-tagged KBTBD7 (**e**). **f, g** KBTBD7 ubiquitinates DRD2. KBTBD7 increased DRD2 ubiquitination in HEK293T cells expressing KBTBD7-Myc, DRD2-Flag, or HA-Ub as indicated (**f**). The level of DRD2 ubiquitination decreased upon knockdown of KBTBD7 and KBTBD6 in HEK293T cells expressing shKBTBD6/7, DRD2-Flag, or HA-Ub as indicated (**g**)

Prolactin secretion analysis

MMQ cells or primary pituitary adenoma cells were infected with KBTBD7 lentivirus or shKBTBD6/7 adenoviruses at 10 MOI. And then, 20000 MMQ cells or primary cells were seeded in triplicate in 96-well plates treated with or without CAB. The supernatants of 2×10^3 MMQ cells or primary cells from prolactinomas were collected. Then, the supernatants were centrifuged at 3000 rpm for 20 min, and the PRL levels in the supernatants were determined using ELISA kits from Haling Biological Technology Co. (Shanghai, HLE20710, China) and Panchao Biological Technology Co. (Shanghai, PCDBH0363, China). For rat prolactinoma model or mice (8–10 weeks), the serum was extracted from the blood and centrifuged 20 min at the speed of 2000 rpm. The PRL levels were determined using ELISA kits from Haling Biological Technology Co. (Shanghai, HLE20710/HLE30489, China).

Rat prolactinoma model

All animal work was approved by the Animal Care Committee of Capital Medical University in accordance with the Institutional Animal Care and Use Committee guidelines. To develop the rat prolactinoma model, rat pituitary tumors were induced by subcutaneously implanting 1-cm silastic capsules containing 10 mg of 17- β estradiol in Fischer 344 rats (female, 4 weeks old). The prolactinomas were induced by 17 β -estradiol, as described in our previous reports [57]. Five weeks later, all the prolactinomas were validated via MRI before intra-pituitary injection. The rats were anaesthetized with an intraperitoneal injection of 10% chloral-durate (3.5 ml/kg), after which 1 μ l of an adenovirus vector expressing KBTBD7 (10^{11} /ml) or the vector control was stereotactically injected into each tumor bilaterally. Tumors were injected at sites relative to the bregma (5.4-mm posterior, 9.6-mm ventral, and 0.8-mm right or left of the bregma) with the tip of a 26-gauge needle fitted to a 10- μ l syringe. The animals were randomly assigned to four groups, and the tumors were allowed to grow to ~ 50 mm 3 in size. At this point, vehicle or CAB (0.5 mg/kg) in 100 μ l of 0.9% saline was administered twice a week by gavage. Two weeks later, after MRI examination to measure the tumor size, all the rats were sacrificed, and tumor tissues and sera were collected for further assessments. The weights of the rat prolactinomas are provided in Suppl. Table 5.

Pituitary tumor samples

Human pituitary tumor tissue samples were obtained from pituitary tumor patients who underwent surgery between 2015 and 2019 at the Department of Neurosurgery, Center of Pituitary Tumor, Ruijin Hospital of Shanghai Jiaotong

University (patient information is provided in Suppl. Tables 6, 7, and 8). This study involving human subjects was approved by the Ethics Committee of the Shanghai Jiao Tong University School of Medicine. Written, informed consent was obtained from all patients whose tumor tissues were used in this study. Consistent with other reports, resistance was defined as the failure of prolactin levels to normalize despite the administration of more than 15 mg of BRC daily or 3 mg of CAB weekly for at least 3 months (a normal PRL level is defined as less than 25 ng/ml). Thirteen dopamine-resistant and twenty-one dopamine-sensitive patients with prolactinoma were examined in this study, as described in our previous report [60]. The 21 dopamine-sensitive patients took BRC and/or CAB after surgical excision and subsequently achieved PRL normalization.

Statistics

All data were presented as the means \pm SD and were analyzed using GraphPad Prism version 7 (GraphPad Software, La Jolla, CA, USA). Unpaired, two-tailed Student's *t* test with a 95% confidence interval was used to analyze data involving the direct comparison of an experimental group with a control group. The reported *p* values were adjusted to account for multiple comparisons. Statistical significance was indicated by *p* < 0.05 and denoted in figures by one asterisk (*p* < 0.05), two asterisks (*p* < 0.01), or three asterisks (*p* < 0.001).

Results

DRD2 is degraded through the ubiquitin-proteasome pathway

To examine the ubiquitination status of DRD2, an *in vivo* ubiquitination assay was performed, and the endogenous DRD2 protein did seem to undergo ubiquitination (Fig. 1a). Furthermore, CAB, a high-affinity DRD2 agonist, appeared to promote the ubiquitination of DRD2 (Fig. 1a). As shown in Fig. 1b, an intracellular segment of DRD2 in fusion with a Flag tag (Flag-DRD2) was also found to be ubiquitinated, which could be further promoted upon CAB treatment (Fig. 1c). To examine the effect of ubiquitination on the stability of DRD2 protein, a CHX (cycloheximide)-based chase experiment was performed. In the presence of 100 μ g/ml CHX, a protein synthesis inhibitor, DRD2 protein, seemed to be degraded fast. However, simultaneous treatment with 20 μ M MG132 was able to prevent DRD2 from degradation (Fig. 1d), indicating that endogenous DRD2 might undergo proteasome-dependent degradation. Similarly, the protein level of Flag-DRD2 was also reduced with CHX treatment, which could also be reversed by MG132 (Fig. 1e).

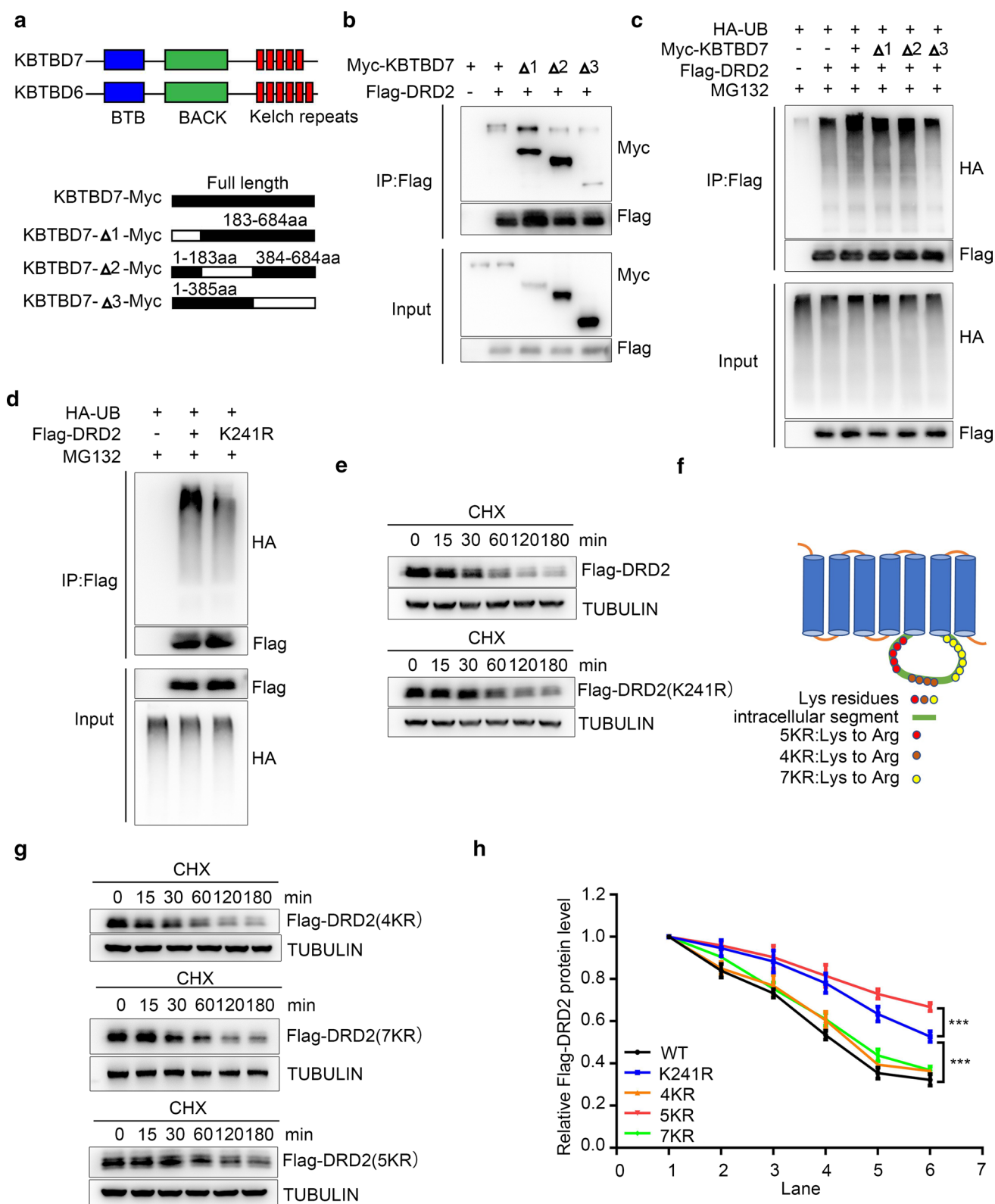


Fig. 3 KBTBD7 activity is dependent on the Kelch structural domain. **a** Schematic representation of KBTBD6 and KBTBD7. **b** Three KBTBD7 deletion constructs interacted with the DRD2 protein. Co-IP experiments were performed with Flag-tagged DRD2 and Myc-tagged full-length KBTBD7 or Myc-tagged KBTBD7 deletion mutants co-expressed in HEK293T cells. **c** Ubiquitination assay in cells co-transfected with DRD2 and different KBTBD7 constructs. Deletion of the Kelch domain from aa 386–684 in KBTBD7 (KBTBD7-Δ3) significantly reduced the ubiquitination of DRD2 compared with that observed in cells expressing full-length KBTBD7. **d** The ubiquitination level of Flag-DRD2 with the K241K mutation was significantly decreased compared to that of WT Flag-tagged DRD2. **e** The K241 mutation increased the stability of DRD2 treated with CHX in HEK293T cells. **f** A map of different mutations from lysine to arginine in Flag-DRD2. **g, h** The K5 mutation increased the half-life of tagged DRD2, as shown in a pulse-chase assay. Flag-DRD2 with different mutations from lysine to arginine were expressed in HEK293T cells treated with CHX. The data are presented as the means \pm SEM. *** $n=3$, $p<0.001$

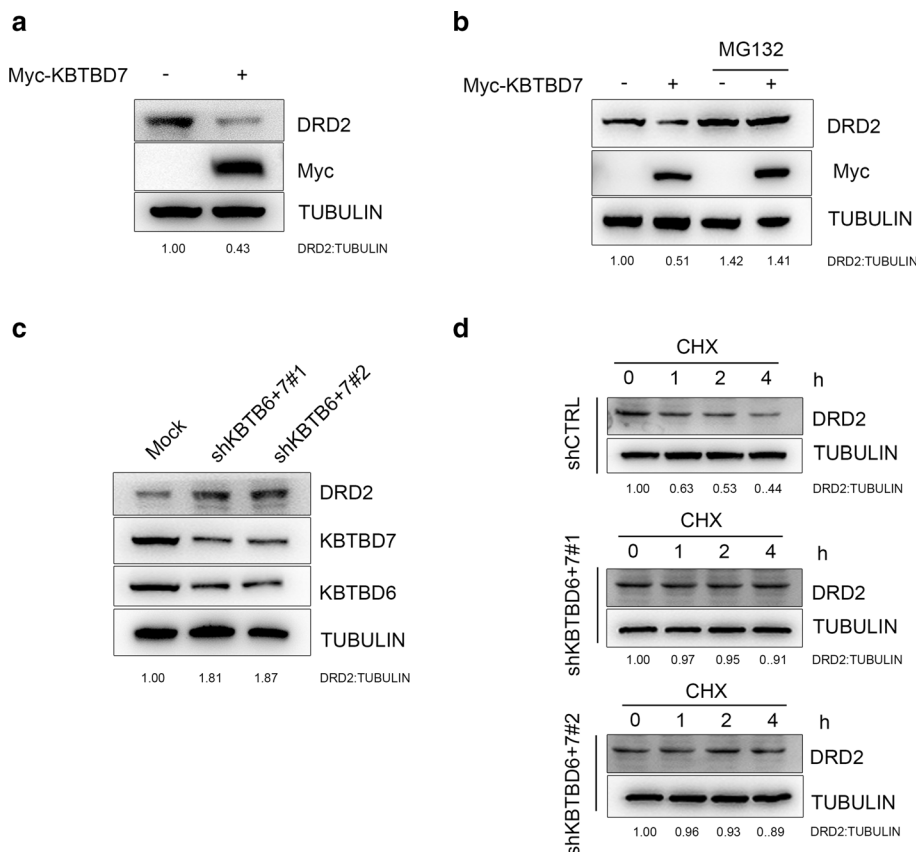
Altogether, endogenous DRD2 protein appeared to be degraded in a proteasome-dependent manner.

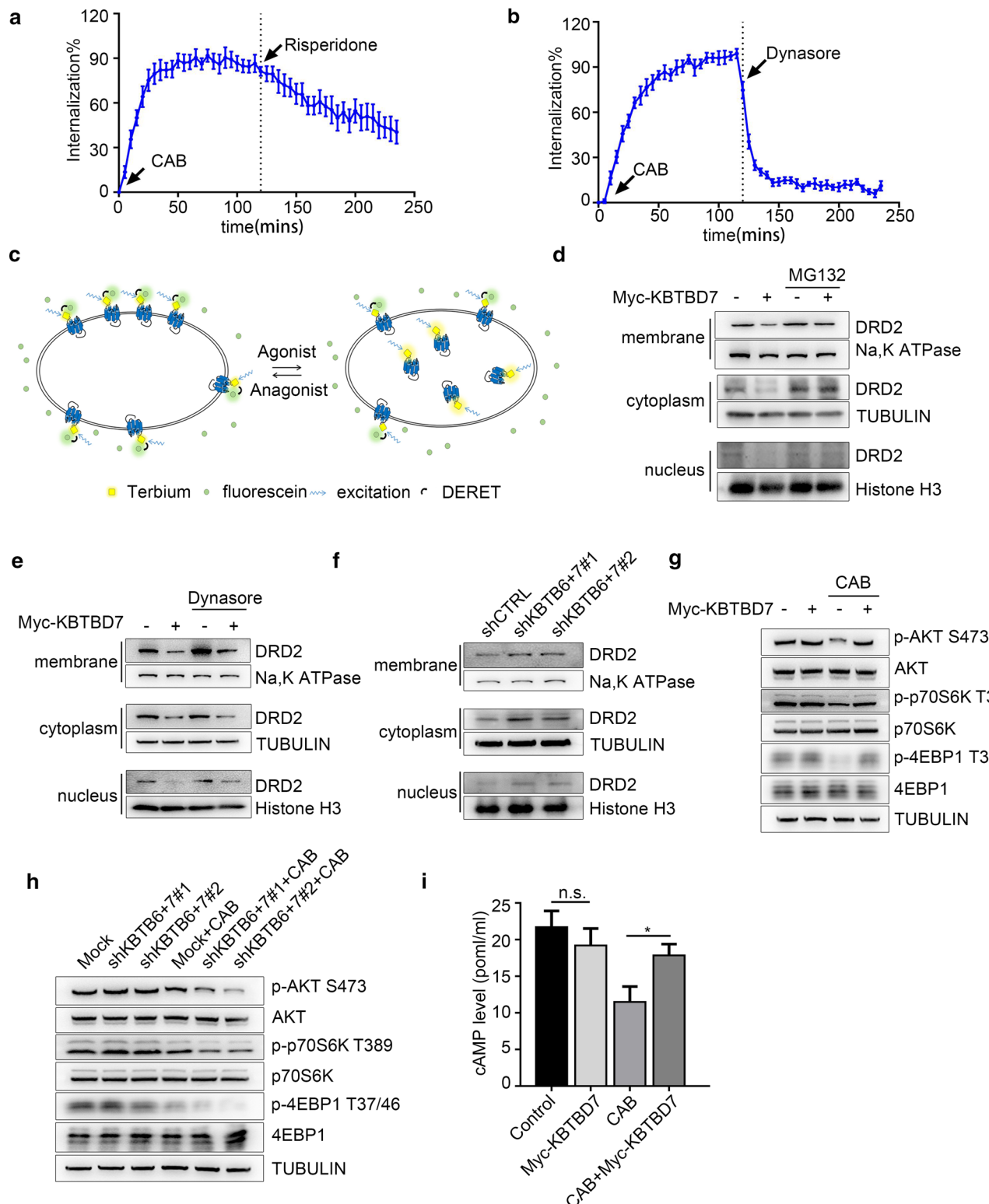
KBTBD7 directly interacts with, and ubiquitinates DRD2

We next attempted to identify the E3 Ub ligase that interacts with DRD2. To this end, a yeast two-hybrid (Y2H) screen was performed to identify the E3 ligase responsible for

DRD2 ubiquitination. Human DRD2 was used as the bait to screen potential DRD2-interacting proteins from a Y2H prey library containing open-reading frames (ORFs) from human cDNAs encoding over 400 putative ubiquitin ligases or their substrate-binding subunits [33, 43]. A KBTBD7–DRD2 interaction was indicated by colony formation on yeast SD-Leu-Trp-His-Ura (SD-4) selection media as well as plate assays for β -galactosidase activity (Fig. 2a). Coimmunoprecipitation (co-IP) analysis indicated that tagged KBTBD7 proteins interacted with the intracellular segment of DRD2 in HEK293T cells (Fig. 2b). Consistently, binding between the endogenous KBTBD7 and DRD2 proteins was observed in HEK293T cells by co-IP analysis, using anti-DRD2 antibody (Fig. 2c). Immunofluorescence microscopy analyses indicated that the Flag-DRD2 and Myc-KBTBD7 proteins, visualized with their respective tagged antibodies, were colocalized in MMQ cells (Fig. 2d). Furthermore, in an in vitro glutathione S-transferase (GST) pulldown assay using recombinant GST-DRD2 and KBTBD7-His proteins, KBTBD7 bound Flag-DRD2, suggesting a direct interaction between these proteins (Fig. 2e). Importantly, to determine whether KBTBD7 promoted Flag-DRD2 ubiquitination, KBTBD7 was overexpressed in HEK293T cells pretreated with MG132 to block proteasome-dependent degradation, which caused a marked accumulation of ubiquitinated Flag-DRD2 (Fig. 2f).

Fig. 4 KBTBD7 downregulates DRD2 expression. **a** The protein level of DRD2 was decreased after KBTBD7 overexpression in HEK293T cells. Cells transfected with Myc-KBTBD7 were cultured for 48 h. **b** A reduction in DRD2 levels due to KBTBD7 overexpression was dependent on proteasomal degradation. Cells transfected with Myc-KBTBD7 were cultured for 48 h and treated with MG132 (20 μ M) for another 6 h. **c** KBTBD6 and KBTBD7 knockdown using shRNAs increased DRD2 protein levels in HEK293T cells. HEK293T cells were infected with efficient lentiviral KBTBD6 and KBTBD7 shRNA or a control shRNA. **d** KBTBD6 and KBTBD7 knockdown prevented DRD2 degradation under CHX treatment, blocking protein synthesis in HEK293T cells





KBTBD7 is a substrate adaptor for the CUL3-RING ubiquitin ligase complex, which also contains another substrate adaptor, KBTBD6 [14]. We observed that KBTBD6 could also interact with DRD2 and increase the ubiquitination of Flag-DRD2 (Suppl. Fig. 1a–e). In addition, two shRNAs

targeting KBTBD7 or KBTBD6, each shown to efficiently and specifically reduce the expression of the target gene at both mRNA and protein levels. Furthermore, knockdown of KBTBD7 and KBTBD6 decreased the ubiquitination of Flag-DRD2 (Fig. 2g, Suppl. Fig. 2a, b).

Fig. 5 KBTBD7 ubiquitinates internalized DRD2 and attenuates the CAB-mediated inhibitory effect on the AKT/mTOR pathway. **a** Internalization was measured in real time using SNAP-DRD2-transfected HEK293 cells. DRD2 was rapidly internalized upon exposure to CAB (10 µM), and DRD2 then returned to the membrane after the addition of risperidone (10 µM). **b** CAB-mediated DRD2 internalization was blocked with the endocytosis inhibitor dynasore (50 µM). **c** Schematic representation of the internalization of DRD2. **d** KBTBD7 overexpression enhanced the degradation of DRD2, interfering with the return of DRD2 to the membrane in HEK293T cells. Cells transfected with Myc-KBTBD7 were cultured for 48 h and treated with MG132 (20 µM) for another 6 h, and Minute™ kits were used for protein extraction and cell fractionation. **e** The degradation of DRD2 was blocked by dynasore. Cells transfected with Myc-KBTBD7 were cultured for 48 h and treated with dynasore (50 µM) for another 6 h, and Minute™ kits were used for protein extraction and cell fractionation. **f** Reduced KBTBD6/7 resulted in DRD2 upregulation on the membrane and in the cytoplasm and nucleus. Cells transfected with Myc-KBTBD7 were cultured for 48 h, and Minute™ kits were used for protein extraction and cell fractionation. **g** KBTBD7 weakened the inhibitory effect of CAB on the AKT/mTOR pathway. Cells transfected with Myc-KBTBD7 were cultured for 48 h and treated with CAB (50 µM) for another 24 h. **h** Reduced KBTBD6/7 enhanced the inhibitory effect of CAB on the AKT/mTOR pathway. Cells transfected with shKBTBD6/7 were cultured for 48 h and treated with CAB (50 µM) for another 24 h. **i** KBTBD7 weakened the inhibitory effect of CAB (20 µM) treatment for 2 h at the cAMP level. The data are presented as the means ± SEM. ***n*=3, *p*<0.01

Altogether, these data clearly indicated that KBTBD6/7 not only directly interacted with the DRD2 protein, but also mediated the ubiquitination of DRD2.

KBTBD7 activity is dependent on its Kelch domain, and KBTBD7 negatively regulates DRD2 at multiple sites

Next, we mapped the DRD2-interacting domains in KBTBD6/7. As shown in Fig. 3a, the structural similarity between KBTBD7 and KBTBD6 is very high. Co-IP experiments were performed with Flag-tagged DRD2 and different deletion mutants of Myc-tagged KBTBD7 that were co-expressed in HEK293T cells. Three KBTBD7 deletion constructs interacted with the DRD2 protein (Fig. 3b). However, deletion of the Kelch domain from aa 386–684 from KBTBD7 (KBTBD7-Δ3) significantly reduced the ubiquitination of DRD2 compared with that of DRD2 upon its co-expression with full-length KBTBD7 or either of the two other deletion mutants examined (Fig. 3c). Consistently, three KBTBD6 deletion constructs could interact with the DRD2 protein. Deletion of the Kelch domain from aa 386–674 from KBTBD6 (KBTBD6-Δ3) significantly reduced the ubiquitination of DRD2 compared with that of DRD2 co-expressed with full-length KBTBD6 or either of the two other deletion mutants examined (Suppl. Fig. 3a–c). These data suggest that the Kelch domains in KBTBD7 and KBTBD6 are critical for their binding and ubiquitin ligase activity towards DRD2.

Previously, Kim et al. reported that ubiquitination at K241 site of wild-type (WT) DRD2 was critical to its degradation [25]. Indeed, the ubiquitination of Flag-DRD2 with the K241 mutation was significantly decreased, compared to that of wild-type Flag-DRD2 (Fig. 3d). In addition, we observed that the mutation of K241 increased the stability of Flag-DRD2 treated with CHX (Fig. 3e). However, as this mutation only partially reversed the degradation of Flag-DRD2, we hypothesized that Flag-DRD2 might contain additional sites for ubiquitination. Totally, there are 16 lysine (Lys) residues, all being potential sites for ubiquitination, in Flag-DRD2. Experiments were performed with different Flag-DRD2 mutants expressed in HEK293T cells in the presence of CHX, the results of which showed that the 5KR mutation enhanced the stability of Flag-DRD2 even more strongly than that by the K241 mutant of flag-DRD2. However, the stability of the 4KR and 7KR mutants was not significantly different from that of WT Flag-DRD2 (Fig. 3f–h).

Collectively, these results indicated that KBTBD6/7 targets DRD2 for degradation through mediating ubiquitination at five sites: K221, K226, K241, K251, and K258.

KBTBD7 downregulates endogenous DRD2 protein

To determine whether KBTBD7 regulates the stability of DRD2, we overexpressed KBTBD7 and observed that the level of DRD2 protein was decreased in HEK293T cells (Fig. 4a). However, when MG312 was used to block proteasome activity, this decrease in the DRD2 protein level upon KBTBD7 overexpression was reversed (Fig. 4b). Consistently, immunoblotting (IB) analyses confirmed that the reduction in KBTBD6/7 resulted in DRD2 upregulation in HEK293T cells (Fig. 4c). In addition, CHX (200 µg/ml) was added at 72 h after infection with shKBTBD6/7 to block protein synthesis, and the level of endogenous DRD2 protein was then determined by immunoblotting analysis. Upon KBTBD6/7 knockdown, the half-life of DRD2 in HEK293T cells was significantly extended compared to that of the control groups (Fig. 4d).

Therefore, KBTBD6/7 seemed to negatively regulate DRD2 protein stability in a proteasome-dependent manner.

KBTBD7 degrades the internalized DRD2 and attenuates CAB-mediated inhibition of the AKT/mTOR pathway

Many GPCRs undergo agonist-mediated endocytosis, a process that may result in the termination of intracellular signaling [16, 22]. However, it remained unknown whether DRD2 undergoes DA-mediated internalization. Using diffusion-enhanced resonance energy transfer (DERET), we observed the rapid internalization of DRD2 upon exposure to CAB,

with D₂R returning to the membrane after the addition of the antagonist risperidone (Fig. 5a). Furthermore, CAB-mediated D₂R internalization could be blocked by dynasore, an endocytosis inhibitor (Fig. 5b). A schematic of D₂R internalization and recycling is shown in Fig. 5c. Using Minute™ kits for protein extraction and cell fractionation, we observed that KBTBD7 could downregulate the expression of D₂R on the membrane and in the cytoplasm and nucleus. When cells were treated with MG312, this decrease in D₂R protein levels upon KBTBD7 overexpression was reversed in the cytoplasm and nucleus, but only partially reversed on the membrane. KBTBD7 ubiquitinated the internalized D₂R, and ubiquitin-modified D₂R could not return to the membrane (Fig. 5d). In addition, after treatment with dynasore, the decrease in D₂R protein levels upon KBTBD7 overexpression was also reversed in the membrane and nucleus (Fig. 5e). This finding indicated that both membrane-localized D₂R and the internalized D₂R could be degraded in a proteasome-dependent manner. Consistently, IB analyses confirmed that knockdown of KBTBD6/7 resulted in D₂R upregulation on the membrane and in the cytoplasm and nucleus (Fig. 5f).

Protein kinase B (AKT) is a signaling molecule downstream of D₂R activation [27], and in our previous study, CAB was shown to inhibit the AKT/mammalian target of rapamycin (mTOR) pathway [57]. To elucidate the pathway downstream of D₂R ubiquitination, we focused on the PI3K/AKT/mTOR pathway. KBTBD7 overexpression did not affect the AKT/mTOR pathway. However, with CAB treatment, KBTBD7 could attenuate inhibition of AKT phosphorylation as well as that of 4E-BP1, although much less on p70S6K, two key downstream effectors of the mTOR pathway (Fig. 5g). In contrast, downregulation of KBTBD6/7 enhanced the inhibition of AKT and 4E-BP1 phosphorylation under CAB treatment (Fig. 5h). Activation of D₂R by DA agonists reduced the production of the soluble second messenger cyclic AMP (cAMP) [37]. KBTBD7 appeared to weaken CAB-induced decrease in the level of cAMP, while the knockdown of KBTBD6/7 had the opposite effect (Fig. 5i, Suppl. Fig. 4a).

Therefore, CAB induced internalization of D₂R and KBTBD7 negatively regulated the stability of membrane-associated and internalized D₂R protein, while alleviating CAB-mediated inhibition of the activity of AKT/mTOR pathway.

Knockout of KBTBD7 increases D₂R protein expression in KBTBD7^{-/-} KO mice

To further address the physiological significance of KBTBD7-mediated ubiquitination and degradation of D₂R at organism level, a KBTBD7 knockout (KO) mouse was generated using the CRISPR-Cas9 technique

(Fig. 6a, b). First, genotyping with PCR was performed to confirm that *KBTBD7* gene was indeed knocked out in KBTBD7^{-/-} mice (Fig. 6c). To determine whether KBTBD7 ablation did stabilize D₂R proteins, we examined D₂R protein levels in the pituitary glands of both KBTBD7-deficient and WT mice, and observed that pituitary D₂R levels were increased in KBTBD7-deficient mice (Fig. 6d). As the expression of D₂R was very important for the secretion of PRL, we determined the plasma PRL level using ELISA, and found that KBTBD7^{-/-} mice had lower PRL secretion compared to WT mice (Fig. 6e).

Furthermore, we tested the D₂R levels in a variety of other organs, including brain, heart, lung, and liver. We observed that D₂R protein was more highly expressed in the brain, especially in the striatum, in KBTBD7^{-/-} mice than in WT mice (Fig. 6f, g). In addition, in the hearts, lungs, livers, and stomachs of KBTBD7-deficient mice, D₂R protein levels were significantly higher than those of WT mice. However, in the spleen and large intestine, D₂R protein levels were not significantly different between the WT and KO mice (Suppl. Fig. 5a, b).

KBTBD7 regulates pituitary tumor sensitivity to DA treatment

Clinically, CAB is the first-line choice for treating prolactinomas. In our previous studies, D₂R was shown to play a critical role in the efficacy of DA treatment for prolactinomas [31, 56]. Then, we went on to ask what role KBTBD7 might play in the DA treatment of PAs. As shown in Fig. 7a, KBTBD7 overexpression downregulated the protein level of D₂R in MMQ cells (Fig. 7a) and significantly increased the resistance of MMQ cells to CAB (Fig. 7b). Furthermore, KBTBD7 overexpression increased MMQ cell colony formation upon CAB treatment (Fig. 7c). To further investigate the function of KBTBD6/7 in pituitary tumor cells, both endogenous KBTBD6 and 7 were stably knocked down in MMQ cells using lentiviral small hairpin RNAs (shRNAs) (Suppl. Fig. 2c, d). In contrast to the KBTBD7 overexpression results, KBTBD6/7 knockdown in MMQ cells with respective shRNA upregulated D₂R expression, increased the sensitivity of MMQ cells to CAB, and inhibited colony formation under CAB treatment (Suppl. Fig. 6a–c). The combined treatment with CAB and dynasore significantly increased MMQ cell suppression compared to that observed following treatment with CAB or dynasore alone (Fig. 7d). Meanwhile, the combined treatment of bortezomib (BTZ), a proteasome inhibitor, with CAB seemed to synergistically suppress the proliferation of MMQ cells, compared to that treated with CAB or BTZ alone (Fig. 7e).

In addition, primary pituitary tumor cells were infected with adenovirus to decrease KBTBD6/7 expression. The primary pituitary tumor cells were derived from twelve patients

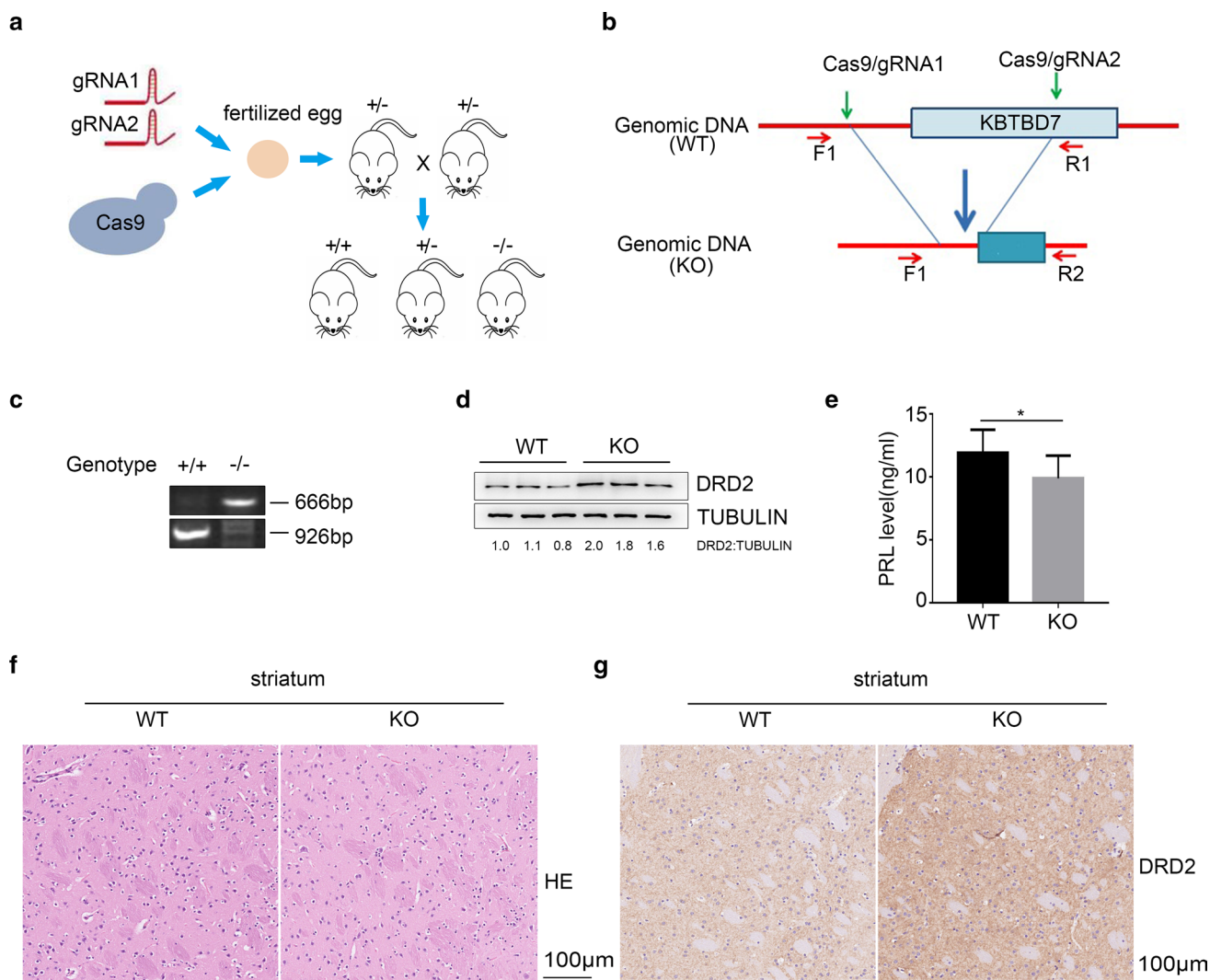
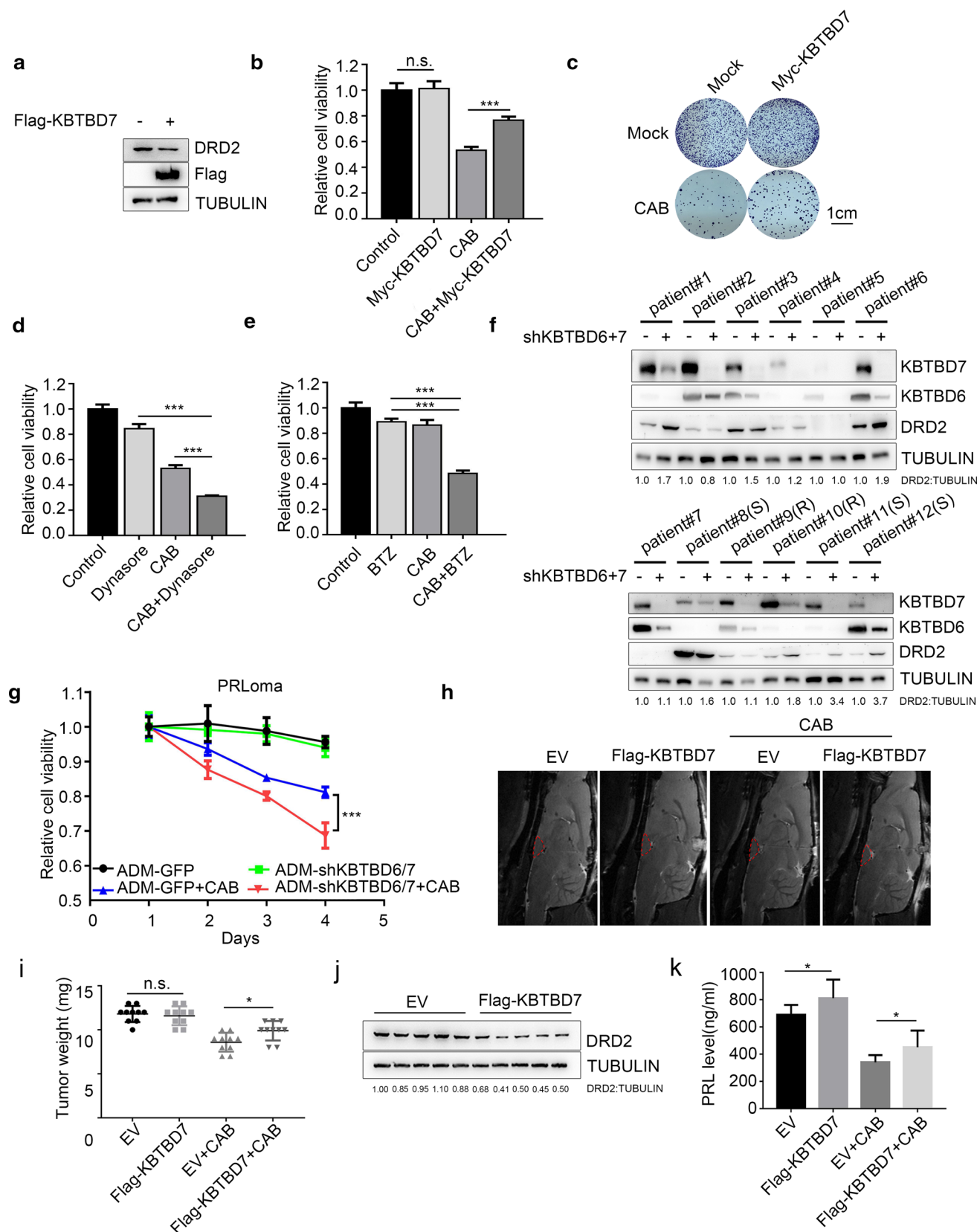


Fig. 6 Knockout of KBTBD7 stabilizes the DRD2 protein in mice. **a** Generation of KBTBD7 KO mice using the Cas9 system. **b** Schematic overview of the strategy used to identify KBTBD7 KO mice. The PCR primers used for genotyping are indicated by arrows. **c** DNA-PAGE images from PCR genotyping of the offspring of intercrossed KBTBD7[±] mice. **d** Knockout of KBTBD7 increased the DRD2 expression in pituitary glands. Pituitary glands were homogenized in lysis buffer with a tissue homogenizer; then, the samples

were centrifuged, and the supernatant was collected and used for immunoblot analysis with the indicated antibodies. **e** Knockout of KBTBD7 inhibited the PRL secretion in mice. Serums were isolated from mice blood, and PRL levels were detected by ELISA kit. * $n=10$, $p<0.05$. **f** Hematoxylin–eosin (HE) staining of the striatum. Scale bar, 100 µm. **g** Representative IHC staining images showed that DRD2 expression was increased in the striatum of KBTBD7^{−/−} mice compared with WT mice. Scale bar, 100 µm

with PAs of different subtypes: five PRL-secreting adenomas, five non-functioning PAs (NFPAs), and two growth hormone (GH)-secreting adenomas. The clinical data of these patients are shown in Suppl. Table 6. Knockdown of KBTBD6/7 seemed to up-regulate the levels of DRD2 protein in most patient-derived cells (Fig. 7f) while sensitizing them to CAB treatment (Fig. 7g, Suppl. Fig. 7a, b). KBTBD6/7 knockdown was found to increase tumor sensitivity to CAB by approximately 71.4% among all primary pituitary tumor cells (100% in PRL-secreting adenomas, 40% in NFPAs, and 50% in GH-secreting adenomas). However, knockdown of the KBTBD6/7 protein levels in four

primary pituitary tumor cells (three from NFPAs and one from GH-secreting adenoma) had no significant effect on the sensitivity of the cells to CAB. Among these cells, although DRD2 was decently expressed in that from patient No. 2, primary pituitary tumor cells from this patient seemed to be resistant to CAB. In addition, patient No. 4 exhibited very low KBTBD6/7 expression, and KBTBD6/7 knockdown had no obvious effect on DRD2 protein levels. Patient No. 5 and 7 exhibited low and no DRD2 expression, respectively, which may have been due to the low transcription of DRD2 mRNA and not the high expression of its E3 ligase, leading to its ubiquitination-mediated degradation.



◀Fig. 7 KBTBD7 regulates the sensitivity of pituitary tumors to DAs. **a** KBTBD7 downregulated the stability of DRD2 in MMQ cells. Cells transfected with Myc-KBTBD7 were cultured for 48 h. **b** KBTBD7 increased the resistance of MMQ cells to CAB. MMQ cells were infected with lentiviral Myc-KBTBD7 or a control plasmid and cultured in the presence or absence of 50 μ M CAB for 48 h, after which cell survival was determined by CCK8 assay. The data are presented as the means \pm SEM. *** $n=4$, $p<0.001$. **c** Colony formation assays showed that KBTBD7 overexpression enhances the colony formation rate in MMQ cells treated with CAB (50 μ M). One thousand cells per well were seeded into 6-well plates and cultured for 12 days, followed by crystal violet staining and colony counting. Scale bar, 1 cm. **d** Combined treatment with CAB (50 μ M) and dynasore (25 μ M) significantly increased MMQ cell suppression compared to that following treatment with CAB or dynasore alone. **e** Combined treatment with BTZ (2 nM) and CAB (25 μ M) significantly increased MMQ cell suppression compared to that observed following treatment with CAB or BTZ alone. **f, g** KBTBD6 and KBTBD7 double knockdown increased the protein level of DRD2 and the sensitivity of primary pituitary tumor cells to CAB. Primary pituitary tumor cells were infected with adenovirus to knock down KBTBD6/7 in the presence or absence of 50 μ M CAB, and cell viability was detected by CCK8 assay. Prolactinomas were labeled with sensitivity (S) or resistance (R). The data are presented as the means \pm SEM. *** $n=4$, $p<0.001$. **h, i** KBTBD7 adenovirus infection reduced therapeutic effects on rat *in situ* prolactinomas. After prolactinomas had been induced with 17 β -estradiol for 6 weeks, tumor-bearing rats were treated with one stereotactic intratumoral injection of 1.0×10^{11} PFU of adenovirus harboring the Flag-KBTBD7 overexpression construct or control EV. After treatment with CAB (0.5 mg/kg/day), tumor masses were measured by MRI (**h**), after which the tumors were then dissected, and the tumor weight was calculated. The data are presented as the means \pm SEM. * $n=10$, $p<0.05$ (**i**). **j** Overexpression of KBTBD7 decreased DRD2 protein levels in rat *in situ* prolactinomas. Tumor tissues described in **h** were homogenized in lysis buffer with a tissue homogenizer; then, the samples were centrifuged, and the supernatant was collected and used for immunoblot analysis with the indicated antibodies. **k** Overexpression of KBTBD7 increased the PRL secretion in rat *in situ* prolactinomas. Blood serums were isolated from blood of rats, and PRL level were detected by ELISA kit, * $n=10$, $p<0.05$

Previously, it was reported that low concentration of CAB could decrease the PRL level in MMQ cells or primary pituitary adenoma cells [10]. We next assessed the effect of KBTBD7 on PRL secretion using PRL ELISA, in the presence or absence of CAB at different concentrations. Overexpression of KBTBD7 had no obvious effect on PRL levels when CAB was absent; however, upon CAB treatment, KBTBD7 markedly attenuated the inhibitory effect of CAB on PRL levels in MMQ cells (Suppl. Fig. 8a). Consistently, KBTBD6/7 knockdown enhanced the inhibitory effect of CAB on PRL in MMQ cells (Suppl. Fig. 8b). Similar results were also obtained with seven lines of primary prolactinoma cells, in which KBTBD6/7 knockdown also significantly potentiated the inhibitory effect of CAB on PRL in six cases (Suppl. Fig. 8c).

Collectively, these results clearly indicated that knockdown of KBTBD6/7 upregulated the level of DRD2 protein and sensitized pituitary tumors to CAB treatment.

KBTBD7 enhances DA resistance in estrogen-induced rat pituitary tumors

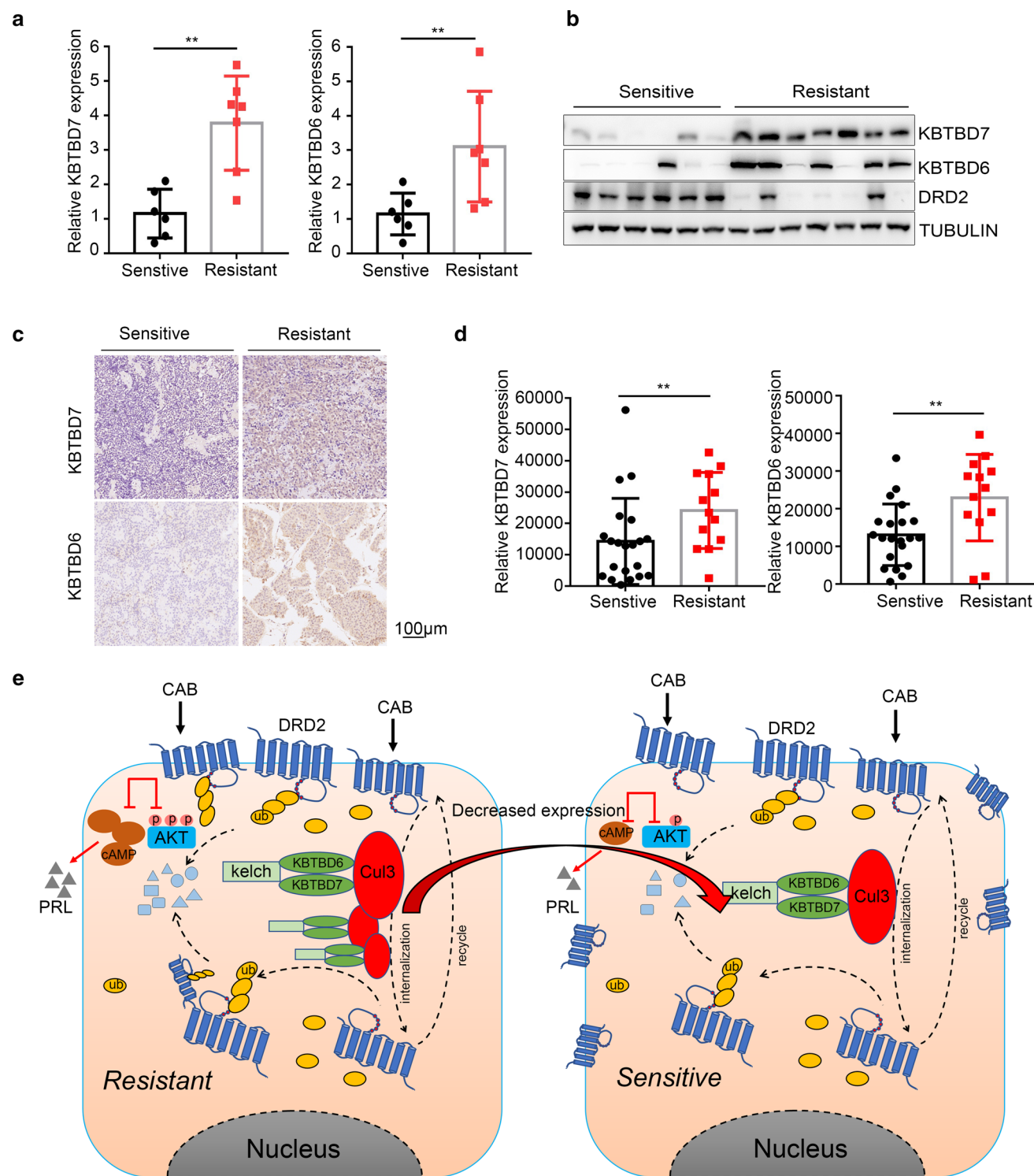
To further test whether KBTBD7-mediated DA resistance is pathophysiologically relevant, an *in situ* rat prolactinoma tumor model was constructed by administering estrogen to Fischer 344 rats as described previously [57]. Rats with hypophysoma, confirmed by magnetic resonance imaging (MRI), were divided into four groups ($n=10$) and administered either adenovirus expressing His-Flag-KBTBD7 or EVs (1×10^{10} PFU, via stereotactic pituitary injection), and two groups were administered CAB. MRI examination showed that the volumes of tumors treated with KBTBD7 adenovirus were not significantly different from those of the control rats treated with EV adenovirus after 14 days. However, tumors treated with KBTBD7 adenovirus and CAB were appreciably heavier than those of the control rats treated with control EV adenovirus and CAB (9.9 ± 0.35 mg vs 8.6 ± 0.34 mg, $p<0.05$, Fig. 7h, i). Furthermore, compared with the tumors from the control EV-infected groups, KBTBD7-infected tumors showed greatly reduced DRD2 expression (Fig. 7j). Overexpression of KBTBD7 increased the PRL levels compared to EV-infected groups, and, accordingly, decreased the inhibitory effect of CAB on PRL levels in rat prolactinoma models (Fig. 7k).

Taken together, these results strongly suggested that KBTBD7 could significantly enhance DA resistance in estrogen-induced *in situ* rat pituitary tumors.

KBTBD7 is a potential biomarker associated with the DA-resistance in prolactinomas to DAs, and is negatively correlated with DRD2 expression

Clinically, approximately 10–20% of prolactinomas are resistant to DA treatment [8, 39]. To understand the clinical significance of KBTBD6/7 in DA efficacy, we compared KBTBD6/7 mRNA expression in DA-sensitive and DA-resistant prolactinomas by quantitative real-time PCR (qRT-PCR). The levels of KBTBD7 and KBTBD6 mRNA in seven DA-resistant prolactinomas were markedly higher than that in six DA-sensitive prolactinomas. However, DRD2 mRNA levels were not significantly different between DA-resistant and DA-sensitive pituitary tumors (Fig. 8a, Suppl. Fig. 9a). Consistently, results from IB analysis clearly showed that KBTBD6/7 protein expression was higher in DA-resistant prolactinomas than in DA-sensitive prolactinomas; however, DRD2 protein expression was lower in DA-resistant prolactinomas than in DA-sensitive prolactinomas (Fig. 8b).

To further confirm these clinical results, immunohistochemical staining analyses were performed with the paraffinized clinical samples that were used and described in our recent study [60]. As shown in Fig. 8c, d, KBTBD7 and KBTBD6 expression was significantly higher in thirteen



DA-resistant prolactinomas than in 21 DA-sensitive prolactinomas, with the clinical data of these patients presented in Suppl. Table 7 and reported before [60]. To further examine the co-relationship between the expression of KBTBD6/7 and DRD2 in pituitary tumors, IHC assays were also carried out to check KBTBD6/7 and DRD2 expression in 109 PAs

[62 NFPAs, 25 PRL-secreting adenomas, 17 GH-secreting adenomas, 3 ACTH (adreno-cortico-trophic-hormone)-secreting tumors, and 2 TSH (thyroid-stimulating hormone)-secreting adenomas], with two representative images in Suppl. Fig. 10a (the clinical data of these patients are shown in Suppl. Table 8). A negative correlation was evident

Fig. 8 Upregulated KBTBD7 is associated with poor prognosis in human prolactinomas. **a** Quantitative real-time PCR and **b** Western blotting results showed that KBTBD7 and KBTBD6 expression was higher in dopamine-resistant prolactinomas ($n=7$) than in sensitive tumors ($n=6$). The data are presented as the means \pm SEM. ** $p < 0.01$. **c** Representative immunohistochemical staining images of KBTBD7 and KBTBD6 in dopamine-sensitive and dopamine-resistant prolactinomas (left and right panels, respectively). Scale bar, 100 μ m. **d** Statistical integrated optical density (sum) of KBTBD7 and KBTBD6 staining in human dopamine-sensitive ($n=21$) and dopamine-resistant prolactinomas ($n=13$). The data are presented as the means \pm SEM. ** $p < 0.01$. **e** A model of KBTBD6/7-mediated DRD2 degradation and its clinical significance. CAB induces internalization of the membrane protein DRD2. When KBTBD6/7 is abundant (left panel, resistant patients), DRD2 on the membrane and internalized DRD2 undergo ubiquitination-mediated degradation, which attenuates CAB-mediated inhibition of the Akt/mTOR pathway, cAMP levels, and PRL levels, increasing pituitary tumor cell survival. In contrast, when KBTBD6/7 is absent in sensitive patients, the ubiquitin-mediated degradation of DRD2 is reduced, and CAB-mediated cell death is enhanced

between the expression levels of KBTBD7 or KBTBD6 and DRD2 in all pituitary tumors examined (Suppl. Fig. 10b). Similar results were also obtained with these prolactinoma adenomas, where there seemed to be yet again a negative correlation between the KBTBD6/7 and DRD2 expression (Suppl. Fig. 10c).

Taken together, KBTBD6/7, whose expression seemed to be negatively correlated with that DRD2 expression in pituitary tumors, was emerging as a novel biomarker potentially associated with the sensitivity of prolactinomas to DAs.

Discussion

In this study, for the first time, we have identified the BTB-Kelch protein KBTBD6/7 as interacting partners for human DRD2 at its third intracellular loop, which regulates the proteasome-dependent degradation of DRD2. Importantly, we elucidate the underlying novel mechanism of PA resistance due to the low expression of DRD2. Clinically, KBTBD6/7 may be an alternative biomarker to predict the drug sensitivity of prolactinomas, while of the potential to become a novel target for the treatment of pituitary tumors (Fig. 8e).

DRs belong to the GPCR superfamily, the largest family of membrane receptors and the most common drug targets [23]. Many known GPCRs, such as β 2-adrenergic receptor [48], the chemokine receptor CXCR4 [35, 36], PAR-1 [55], and PAR-2 [21], have been demonstrated to undergo ubiquitination. Rondou et al. reported that KLHL12 is an adaptor that targets DRD4 ubiquitination. However, KLHL12 was not observed to induce the proteasomal degradation of DRD4 [46, 47, 52]. They also showed that other DR subtypes undergo basal ubiquitination, but this ubiquitination was not affected by KLHL12. Another DR reported to be

ubiquitinated is DRD2, as exogenous DRD2 was shown to be modified by ubiquitination at K241 [25]. However, the study by Ok-Jin Kim did not examine the E3 ligase of DRD2 or the biological/clinical significance of DRD2 ubiquitination. In our study, we identified KBTBD6/7 as an E3 ligase adaptor responsible for the ubiquitination-mediated degradation of DRD2. In addition, we elucidated the sites of DRD2 modified by polyubiquitination and the clinical significance of the regulation of DRD2 ubiquitination.

An increasing body of evidence has established that Ub signaling regulates the chemosensitivity of tumors, although pinpointing the roles of specific Ub signaling pathways in given types of tumors remains challenging. For example, the E3 ubiquitin ligase TRAF6 increases K63-linked ubiquitination and enhances the stability of the antiapoptotic protein MCL1. Thus, IRAK inhibition inactivates the E3 ubiquitin ligase TRAF6, reduces MCL1 stability, and sensitizes T acute lymphoblastic leukemia to combination therapy [32]. TRAF6 ubiquitinates DNMT protein through its E3 ligase activity, leading to lysosome-dependent DNMT protein degradation. Depletion of TRAF6 induces triple-negative breast cancer resistance to decitabine by blocking decitabine-induced DNMT degradation [61]. Mdm2 regulates ubiquitination of the p53 protein, thereby inhibiting the anticancer effect of p53 and promoting the proliferation of breast cancer cells. Furthermore, decreased stability of Mdm2 was observed to promote chemotherapy drug-induced p53-related apoptosis [17, 54]. RNF8 was observed to ubiquitinate Twist and promote its nucleation, thereby increasing the chemosensitivity of breast cancer [28]. Upregulation of FBXW7 was shown to promote CRY2 ubiquitination and increase the chemosensitivity of colon cancer cells [12]. In this study, we clearly demonstrated that the KBTBD6/7 E3 ligase complex regulates the DA sensitivity of pituitary tumors by ubiquitinating DRD2.

Clinically, a number of prolactinoma patients have been shown to be resistant to DA treatment due to the low expression of DRD2. Is there an effective way to potentiate the effect of DA treatment by enhancing endogenous DRD2 protein levels in prolactinoma? GH3 cells express lower levels of DRD2 mRNA than MMQ cells, as the *DRD2* gene exhibits increased CpG island-associated methylation and GH3 cells are enriched in histone H3K27me3, whereas MMQ cells show enrichment for H3K9Ac and barely detectable H3K27me3 [1]. Zebularine and trichostatin A mediate DNA demethylation and the inhibition of histone deacetylation, respectively, and their application resulted in the re-expression of endogenous DRD2 in GH3 cells [58]. Furthermore, Bondioni et al. reported that 9-cis retinoic acid induced re-expression of DRD2 in primary human pituitary tumor cells and GH3 cells [5]. These studies elucidated the mechanism for how the low expression of DRD2 from the perspective of the mRNA translation process and showed

that the decreased endogenous expression of DRD2 following interference with methylation of the promoter region could be upregulated. In our study, we elucidated the cause of the low expression of the DRD2 protein from the perspective of posttranslational protein modification. The proteasome inhibitors bortezomib and ixazomib were recently used to treat multiple myelomas by inhibiting the proteasome [40, 41, 45]. The results of our study clearly demonstrate the potential benefits of combined CAB and BTZ treatment in pituitary tumor growth suppression, and provides a rationale for conducting pilot clinical studies of this combination therapy for human pituitary tumors.

DRD2 plays an important role in human memory/activity, PAs, and craniocerebral diseases [3, 9, 11, 13, 24, 26, 30, 37, 49, 50]. When KBTBD7 was knocked out in mice, we observed that the expression of DRD2 was increased in the normal pituitary gland, as expected. In addition, the expression of DRD2 was increased in the brain, primarily in the striatum and thalamic nucleus. KBTBD7 is highly evolutionarily conserved and may be important in development and disease [20]. KBTBD has an unusual strain-specific expression pattern in the mouse brain and is likely involved in learning and memory. In addition, KBTBD7 may have a specific role in brain development and function [34]. The results of this study provide reasonably strong support for the notion that KBTBD6/7-mediated DRD2 ubiquitin may be involved in these important functions in the brain. Furthermore, KBTBD7 was shown to promote the activation of p38 and NF- κ B signaling by interacting with MKK3/6, resulting in reduced survival rates and cardiac function and increased infarct and scar sizes after myocardial infarction [59]. Interestingly, we also observed that the expression of DRD2 was increased in a variety of different organs, including the heart, in a KBTBD7 KO mouse model. Thus, our findings provide a basis for future exploration of the function of the KBTBD6/7–DRD2 interaction.

Acknowledgements This work was supported by the National Natural Science Foundation of China under Grant Number 81972339 and 81671371 (ZBW), Shanghai Municipal Science and Technology Commission 18XD1403400 (ZBW), Program of Shanghai Academic Research Leader (ZBW), and Shanghai Training and Support Program for Outstanding Young Medical Talents (ZBW). This work was supported by funding to RH from the Strategic Priority Research Program of the Chinese Academy of Sciences (XDB19000000 and XDA12040323), the National Science Foundation of China (91853128, 31470770, and 81525019), the model animal project of Shanghai Science and Technology Commission (19140903500), the Ministry of Science and Technology of China (2019YFA082103 and 2018ZX10101004), Shanghai Municipal Science and Technology Major Project (2017SHZDZX01), and Shenzhen-Hong Kong Institute of Brain Science (NYKFKT2019006).

Author contributions YTL, FL, LC, and LX performed the experiments, analyzed the data, and co-wrote the manuscript. WTG, YZZ, and HT contributed to study of human pituitary adenoma samples. HY,

YZ, WQX, BHR, ZHX, and YJN contributed to the data analysis. YW provided the specimens of pituitary tumours. ZBW and RH conceived the idea, designed and supervised the study, analyzed the data, and co-wrote the manuscript.

Conflict of interest The authors have declared that no conflict of interest exists.

References

- Al-Azzawi H, Yaqub-Usman K, Richardson A, Hofland LJ, Clayton RN, Farrell WE (2011) Reversal of endogenous dopamine receptor silencing in pituitary cells augments receptor-mediated apoptosis. *Endocrinology* 152:364–373. <https://doi.org/10.1210/en.2010-0886>
- Bartrés-Faz D, Martí MJ, Junqué C, Solé-Padullés C, Ezquerre M, Bralten LBC et al (2007) Increased cerebral activity in Parkinson's disease patients carrying the DRD2 TaqIA A1 allele during a demanding motor task: a compensatory mechanism? *Genes Brain Behav* 6:588–592. <https://doi.org/10.1111/j.1601-183X.2006.00290.x>
- Beaulieu JM, Gainetdinov RR (2011) The physiology, signaling, and pharmacology of dopamine receptors. *Pharmacol Rev* 63:182–217. <https://doi.org/10.1124/pr.110.002642>
- Bevan JS, Webster J, Burke CW, Scanlon MF (1992) Dopamine agonists and pituitary tumor shrinkage. *Endocr Rev* 13:220–240. <https://doi.org/10.1210/edrv-13-2-220>
- Bondioni S, Angioni AR, Corbetta S, Locatelli M, Ferrero S, Ferrante E et al (2008) Effect of 9-cis retinoic acid on dopamine D2 receptor expression in pituitary adenoma cells. *Exp Biol Med* 233:439–446. <https://doi.org/10.3181/0704-RM-94>
- Caccavelli L, Feron F, Morange I, Rouer E, Benarous R, Dewailly D et al (1994) Decreased expression of the two D2 dopamine receptor isoforms in bromocriptine-resistant prolactinomas. *Neuroendocrinology* 60:314–322. <https://doi.org/10.1159/000126764>
- Casanueva FF, Molitch ME, Schlechte JA, Abs R, Bonert V, Bronstein MD et al (2006) Guidelines of the Pituitary Society for the diagnosis and management of prolactinomas. *Clin Endocrinol* 65:265–273. <https://doi.org/10.1111/j.1365-2265.2006.02562.x>
- Colao A, Savastano S (2011) Medical treatment of prolactinomas. *Nat Rev Endocrinol* 7:267–278. <https://doi.org/10.1038/nrendo.2011.37>
- Comings DE (1994) Genetic factors in substance abuse based on studies of Tourette Syndrome and ADHD probands and relatives. II. Alcohol abuse. *Drug Alcohol Depend* 35:17–24. [https://doi.org/10.1016/0376-8716\(94\)90105-8](https://doi.org/10.1016/0376-8716(94)90105-8)
- Cuny T, Mohamed A, Graillon T, Roche C, Defilles C, Germanetti AL et al (2012) Somatostatin receptor sst2 gene transfer in human prolactinomas in vitro: impact on sensitivity to dopamine, somatostatin and dopastatin, in the control of prolactin secretion. *Mol Cell Endocrinol* 355:106–113. <https://doi.org/10.1016/j.mce.2012.01.026>
- Duvarci S, Simpson EH, Schneider G, Kandel ER, Roeper J, Sigurdsson T (2018) Impaired recruitment of dopamine neurons during working memory in mice with striatal D2 receptor overexpression. *Nat Commun*. <https://doi.org/10.1038/s41467-018-05214-4>
- Fang L, Yang Z, Zhou J, Tung JY, Hsiao CD, Wang L et al (2015) Circadian clock gene CRY2 degradation is involved in chemoresistance of colorectal cancer. *Mol Cancer Ther* 14:1476–1487. <https://doi.org/10.1158/1535-7163.MCT-15-0030>
- Gallo EF, Salling MC, Feng B, Morón JA, Harrison NL, Javitch JA et al (2015) Upregulation of dopamine D2 receptors in the nucleus accumbens indirect pathway increases locomotion but

- does not reduce alcohol consumption. *Neuropsychopharmacol* 40:1609–1618. <https://doi.org/10.1038/npp.2015.11>
14. Genau HM, Huber J, Baschieri F, Akutsu M, Dötsch V, Farhan H et al (2015) CUL3-KBTBD6/KBTBD7Ubiquitin ligase cooperates with GABARAP proteins to spatially restrict TIAM1-RAC1 signaling. *Mol Cell* 57:995–1010. <https://doi.org/10.1016/j.molcel.2014.12.040>
 15. Gillam MP, Molitch ME, Lombardi G, Colao A (2006) Advances in the treatment of prolactinomas. *Endocr Rev* 27:485–534. <https://doi.org/10.1210/er.2005-9998>
 16. Godbole A, Lyga S, Lohse MJ, Calebiro D (2017) Internalized TSH receptors en route to the TGN induce local Gs-protein signaling and gene transcription. *Nat Commun* 8:443. <https://doi.org/10.1038/s41467-017-00357-2>
 17. Haupt Y, Maya R, Kazaz A, Oren M (1997) Mdm2 promotes the rapid degradation of p53. *Nature* 387:296–299. <https://doi.org/10.1038/387296a0>
 18. Hoeller D, Dikic I (2009) Targeting the ubiquitin system in cancer therapy. *Nature* 458:438–444. <https://doi.org/10.1038/nature07960>
 19. Hollstein PE, Cichowski K (2013) Identifying the ubiquitin ligase complex that regulates the NF1 tumor suppressor and Ras. *Cancer Discov* 3:880–893. <https://doi.org/10.1158/2159-8290.CD-13-0146>
 20. Hu J, Yuan W, Tang M, Wang Y, Fan X, Mo X et al (2010) KBTBD7, a novel human BTB-kelch protein, activates transcriptional activities of SRE and AP-1. *Bmb Rep* 43:17–22. <https://doi.org/10.5483/BMBRep.2010.43.1.017>
 21. Jacob C, Cottrell GS, Gehringer D, Schmidlin F, Grady EF, Bennett NW (2005) c-Cbl mediates ubiquitination, degradation, and down-regulation of human protease-activated receptor 2. *J Biol Chem* 280:16076–16087. <https://doi.org/10.1074/jbc.M500109200>
 22. Jiang X, Huang F, Marusyk A, Sorkin A (2003) Grb2 regulates internalization of EGF receptors through clathrin-coated pits. *Mol Biol Cell* 14:858–870. <https://doi.org/10.1091/mbc.E02-08-0532>
 23. Kebabian JW, Calne DB (1979) Multiple receptors for dopamine. *Nature* 277:93–96. <https://doi.org/10.1038/277093a0>
 24. Kellendonk C, Simpson EH, Polan HJ, Malleret G, Vronskaya S, Winiger V et al (2006) Transient and selective overexpression of dopamine D2 receptors in the striatum causes persistent abnormalities in prefrontal cortex functioning. *Neuron* 49:603–615. <https://doi.org/10.1016/j.neuron.2006.01.023>
 25. Kim OJ (2008) A single mutation at lysine 241 alters expression and trafficking of the D2 dopamine receptor. *J Recept Signal Transduct Res* 28:453–464. <https://doi.org/10.1080/10799890802379410>
 26. Kramer PF, Christensen CH, Hazelwood LA, Dobi A, Bock R, Sibley DR et al (2011) Dopamine D2 receptor overexpression alters behavior and physiology in Drd2-EGFP mice. *J Neurosci* 31:126–132. <https://doi.org/10.1523/JNEUROSCI.4287-10.2011>
 27. Lai WS, Xu B, Westphal KGC, Paterlini M, Olivier B, Pavlidis P et al (2006) Akt1 deficiency affects neuronal morphology and predisposes to abnormalities in prefrontal cortex functioning. *Proc Natl Acad Sci USA* 103:16906–16911. <https://doi.org/10.1073/pnas.0604994103>
 28. Lee HJ, Li CF, Ruan D, Powers S, Thompson PA, Frohman MA et al (2016) The DNA Damage transducer RNF8 facilitates cancer chemoresistance and progression through twist activation. *Mol Cell* 63:1021–1033. <https://doi.org/10.1016/j.molcel.2016.08.009>
 29. Legro RS, Arslanian SA, Ehrmann DA, Hoeger KM, Murad MH, Pasquali R et al (2013) Diagnosis and treatment of polycystic ovary syndrome: an endocrine society clinical practice guideline. *J Clin Endocrinol Metab* 98:4565–4592. <https://doi.org/10.1210/jc.2013-2350>
 30. LeSauter J, Balsam PD, Simpson EH, Silver R (2020) Overexpression of striatal D2 receptors reduces motivation thereby decreasing food anticipatory activity. *Eur J Neurosci* 51:71–81. <https://doi.org/10.1111/ejn.14219>
 31. Li Q, Su Z, Liu J, Cai L, Lu J, Lin S et al (2014) Dopamine receptor D2S gene transfer improves the sensitivity of GH3 rat pituitary adenoma cells to bromocriptine. *Mol Cell Endocrinol* 382:377–384. <https://doi.org/10.1016/j.mce.2013.10.021>
 32. Li Z, Younger K, Gartenhaus R, Joseph AM, Hu F, Baer MR et al (2015) Inhibition of IRAK1/4 sensitizes T cell acute lymphoblastic leukemia to chemotherapies. *J Clin Invest* 125:1081–1097. <https://doi.org/10.1172/JC175821>
 33. Liu Z, Chen P, Gao H, Gu Y, Yang J, Peng H et al (2014) Ubiquitylation of autophagy receptor optineurin by HACE1 activates selective autophagy for tumor suppression. *Cancer Cell* 26:106–120. <https://doi.org/10.1016/j.ccr.2014.05.015>
 34. Makeyev AV, Bayarsaikhan D (2009) New TFII-I family target genes involved in embryonic development. *Biochem Biophys Res Commun* 386:554–558. <https://doi.org/10.1016/j.bbrc.2009.06.045>
 35. Marchese A, Benovic JL (2001) Agonist-promoted ubiquitination of the G protein-coupled receptor CXCR4 mediates lysosomal sorting. *J Biol Chem* 276:45509–45512. <https://doi.org/10.1074/jbc.C100527200>
 36. Marchese A, Raiborg C, Santini F, Keen JH, Stenmark H, Benovic JL (2003) The E3 ubiquitin ligase AIP4 mediates ubiquitination and sorting of the G protein-coupled receptor CXCR4. *Dev Cell* 5:709–722. [https://doi.org/10.1016/S1534-5807\(03\)00321-6](https://doi.org/10.1016/S1534-5807(03)00321-6)
 37. Missale C, Russel Nash S, Robinson SW, Jaber M, Caron MG (1998) Dopamine receptors: from structure to function. *Physiol Rev* 78:189–225. <https://doi.org/10.1152/physrev.1998.78.1.189>
 38. Molitch ME (2002) Medical management of prolactin-secreting pituitary adenomas. *Pituitary* 5:55–65. <https://doi.org/10.1023/a:1022375429083>
 39. Molitch ME (2005) Pharmacologic resistance in prolactinoma patients. *Pituitary* 8:43–52. <https://doi.org/10.1007/s11102-005-5085-2>
 40. Moreau P, Masszi T, Grzasko N, Bahlis NJ, Hansson M, Pour L et al (2016) Oral Ixazomib, lenalidomide, and dexamethasone for multiple myeloma. *N Engl J Med* 374:1621–1634. <https://doi.org/10.1056/NEJMoa1516282>
 41. Palumbo A, Chanan-Khan A, Weisel K, Nooka AK, Masszi T, Beksaç M et al (2016) Daratumumab, bortezomib, and dexamethasone for multiple myeloma. *N Engl J Med* 375:754–766. <https://doi.org/10.1056/NEJMoa1606038>
 42. Passos VQ, Fortes MAHZ, Giannella-Neto D, Bronstein MD (2009) Genes differentially expressed in prolactinomas responsive and resistant to dopamine agonists. *Neuroendocrinology* 89:163–170. <https://doi.org/10.1159/000156116>
 43. Peng H, Yang J, Li G, You Q, Han W, Li T et al (2017) Ubiquitylation of p62/sequestosome1 activates its autophagy receptor function and controls selective autophagy upon ubiquitin stress. *Cell Res* 27:657–674. <https://doi.org/10.1038/cr.2017.40>
 44. Popendikyte V, Laurinavicius A, Paterson AD, Macciardi F, Kennedy JL, Petronis A (1999) DNA methylation at the putative promoter region of the human dopamine D2 receptor gene. *NeuroReport* 10:1249–1255. <https://doi.org/10.1097/00001756-19990426-00018>
 45. Richardson PG, Sonneveld P, Schuster MW, Irwin D, Stadtmauer EA, Facon T et al (2005) Bortezomib or high-dose dexamethasone for relapsed multiple myeloma. *N Engl J Med* 352:2487–2498. <https://doi.org/10.1056/NEJMoa043445>
 46. Rondou P, Haegeman G, Vanhoenacker P, Van Craenenbroeck K (2008) BTB protein KLHL12 targets the dopamine D4 receptor for ubiquitination by a Cul3-based E3 ligase. *J Biol Chem* 283:11083–11096. <https://doi.org/10.1074/jbc.M708473200>
 47. Rondou P, Skierska K, Packeu A, Lintermans B, Vanhoenacker P, Vauquelin G et al (2010) KLHL12-mediated ubiquitination

- of the dopamine D4 receptor does not target the receptor for degradation. *Cell Signal* 22:900–913. <https://doi.org/10.1016/j.cellsig.2010.01.014>
48. Shenoy SK, McDonald PH, Kohout TA, Lefkowitz RJ (2001) Regulation of receptor fate by ubiquitination of activated β 2-adrenergic receptor and β -arrestin. *Science* 294:1307–1313. <https://doi.org/10.1126/science.1063866>
 49. Sibley DR, Monsma FJ (1992) Molecular biology of dopamine receptors. *Trends Pharmacol Sci* 13:61–69. [https://doi.org/10.1016/0165-6147\(92\)90025-2](https://doi.org/10.1016/0165-6147(92)90025-2)
 50. Tabor A, Weisenburger S, Banerjee A, Purkayastha N, Kaindl JM, Hübner H et al (2016) Visualization and ligand-induced modulation of dopamine receptor dimerization at the single molecule level. *Sci Rep UK*. <https://doi.org/10.1038/srep33233>
 51. Takahashi H, Takano H, Kodaka F, Arakawa R, Yamada M, Otsuka T et al (2010) Contribution of dopamine D1 and D2 receptors to amygdala activity in human. *J Neurosci* 30:3043–3047. <https://doi.org/10.1523/JNEUROSCI.5689-09.2010>
 52. Van Tol HHM, Wu CM, Guan HC, Ohara K, Bunzow JR, Civelli O et al (1992) Multiple dopamine D4 receptor variants in the human population. *Nature* 358:149–152. <https://doi.org/10.1038/358149a0>
 53. Varshavsky A (1997) The ubiquitin system. *Trends Biochem Sci* 22:383–387. [https://doi.org/10.1016/s0968-0004\(97\)01122-5](https://doi.org/10.1016/s0968-0004(97)01122-5)
 54. Watson IR, Li BK, Roche O, Blanch A, Ohh M, Irwin MS (2010) Chemotherapy induces NEDP1-mediated destabilization of MDM2. *Oncogene* 29:297–304. <https://doi.org/10.1038/onc.2009.314>
 55. Wolfe BL, Marchese A, Trejo JA (2007) Ubiquitination differentially regulates clathrin-dependent internalization of protease-activated receptor-1. *J Cell Biol* 177:905–916. <https://doi.org/10.1083/jcb.200610154>
 56. Wu ZB, Zheng WM, Su ZP, Chen Y, Wu JS, Wang CD et al (2010) Expression of D2R mRNA isoforms and ER mRNA isoforms in prolactinomas: correlation with the response to bromocriptine and with tumor biological behavior. *J Neuro-Oncol* 99:25–32. <https://doi.org/10.1007/s11060-009-0107-y>
 57. Wu ZR, Yan L, Liu YT, Cao L, Guo YH, Zhang Y et al (2018) Inhibition of mTORC1 by lncRNA H19 via disrupting 4E-BP1/Raptor interaction in pituitary tumours. *Nat Commun* 9:4624. <https://doi.org/10.1038/s41467-018-06853-3>
 58. Yacqub-Usman K, Duong CV, Clayton RN, Farrell WE (2013) Preincubation of pituitary tumor cells with the epidermal growth factor receptor kinase inhibitor zebularine and trichostatin A are permissive for retinoic acid-augmented expression of the BMP-4 and D2R genes. *Endocrinology* 154:1711–1721. <https://doi.org/10.1210/en.2013-1061>
 59. Yang L, Wang B, Zhou Q, Wang Y, Liu X, Liu Z et al (2018) MicroRNA-21 prevents excessive inflammation and cardiac dysfunction after myocardial infarction through targeting KBTBD7. *Cell Death Dis* 9:769. <https://doi.org/10.1038/s41419-018-0805-5>
 60. Yao H, Tang H, Zhang Y, Zhang QF, Liu XY, Liu YT et al (2019) DEPTOR inhibits cell proliferation and confers sensitivity to dopamine agonist in pituitary adenoma. *Cancer Lett* 459:135–144. <https://doi.org/10.1016/j.canlet.2019.05.043>
 61. Yu J, Qin B, Moyer AM, Nowsheen S, Liu T, Qin S et al (2018) DNA methyltransferase expression in triple-negative breast cancer predicts sensitivity to decitabine. *J Clin Invest* 128:2376–2388. <https://doi.org/10.1172/JCI97924>
 62. Zhang Z, Turer E, Li X, Zhan X, Choi M, Tang M et al (2016) Insulin resistance and diabetes caused by genetic or diet-induced KBTBD2 deficiency in mice. *Proc Natl Acad Sci USA* 113:E6418–E6426. <https://doi.org/10.1073/pnas.1614467113>
 63. Wu ZB, Yu CJ, Su ZP, Zhuge QC, Wu JS, Zheng WM (2006) Bromocriptine treatment of invasive giant prolactinomas involving the cavernous sinus: Results of a long-term follow up. *J Neurosurg* 104:54–61. <https://doi.org/10.3171/jns.2006.104.1.54>

Publisher's Note Springer Nature remains neutral with regard to jurisdictional claims in published maps and institutional affiliations.

Affiliations

Yan Ting Liu¹ · Fang Liu^{2,6} · Lei Cao³ · Li Xue¹ · Wei Ting Gu¹ · Yong Zhi Zheng^{1,4} · Hao Tang¹ · Yu Wang⁵ · Hong Yao¹ ·
Yong Zhang¹ · Wan Qun Xie^{1,4} · Bo Han Ren^{1,4} · Zhuo Hui Xiao² · Ying Jie Nie⁶ · Ronggui Hu^{2,7,8} · Zhe Bao Wu^{1,4} 

¹ Department of Neurosurgery, Center of Pituitary Tumor, Ruijin Hospital, Shanghai Jiao Tong University School of Medicine, Shanghai 200025, China

² State Key Laboratory of Systems Biology, CAS Center for Excellence in Molecular Cell Science, Innovation Center for Cell Signaling Network, Shanghai Institute of Biochemistry and Cell Biology, Chinese Academy of Sciences, University of Chinese Academy of Sciences, Shanghai 200031, China

³ Department of Neurosurgery, Beijing Tiantan Hospital, Capital Medical University, Beijing 100070, China

⁴ Department of Neurosurgery, First Affiliated Hospital of Wenzhou Medical University, Wenzhou 325000, China

⁵ Department of Neurosurgery, Renji Hospital, Shanghai Jiao Tong University School of Medicine, Shanghai 200127, China

⁶ Clinical Research Lab Center, Guizhou Provincial People's Hospital, Guiyang 550002, China

⁷ School of Life Science, Hangzhou Institute for Advanced Study, University of Chinese Academy of Sciences, Hangzhou 310024, China

⁸ Guangdong Provincial Key Laboratory of Brain Connectome and Behavior, CAS Key Laboratory of Brain Connectome and Manipulation, the Brain Cognition and Brain Disease Institute (BCBDI), Shenzhen Institutes of Advanced Technology, Chinese Academy of Sciences, Shenzhen-Hong Kong Institute of Brain Science-Shenzhen Fundamental Research Institutions, Shenzhen 518055, China